Progress in Particle and Nuclear Physics 102 (2018) 48–72

Contents lists available at ScienceDirect

Progress in Particle and Nuclear Physics

journal homepage: www.elsevier.com/locate/ppnp

Review

Current unknowns in the three-neutrino framework

F. Capozzi [a], E. Lisi [b,*], A. Marrone [c,b], A. Palazzo [c,b]

[a] Max-Planck-Institut für Physik (Werner-Heisenberg-Institut), Föhringer Ring 6, 80805 München, Germany
[b] Istituto Nazionale di Fisica Nucleare, Sezione di Bari, Via Orabona 4, 70126 Bari, Italy
[c] Dipartimento Interateneo di Fisica dell'Università di Bari, Via Amendola 173, 70126 Bari, Italy

ARTICLE INFO

Article history:
Available online 18 May 2018

Keywords:
Neutrino masses and mixings
Neutrino oscillations
Global data analysis

ABSTRACT

We present an up-to-date global analysis of data coming from neutrino oscillation and non-oscillation experiments, as available in April 2018, within the standard framework including three massive and mixed neutrinos. We discuss in detail the status of the three-neutrino (3ν) mass-mixing parameters, both known and unknown. Concerning the latter, we find that: normal ordering (NO) is favored over inverted ordering (IO) at 3σ level; the Dirac CP phase is constrained within $\sim$ 15% ($\sim$ 9%) uncertainty in NO (IO) around nearly-maximal CP-violating values; the octant of the largest mixing angle and the absolute neutrino masses remain undetermined. We briefly comment on other unknowns related to theoretical and experimental uncertainties (within 3ν) or possible new states and interactions (beyond 3ν).

Contents

* Corresponding author.
E-mail address: eligio.lisi@ba.infn.it (E. Lisi).

https://doi.org/10.1016/j.ppnp.2018.05.005
0146-6410/

1. Introduction

This work represents an ideal follow-up of a previous review in this Journal [1], where a global analysis of oscillation and non-oscillation data as of 2005 was discussed in detail, within the framework of three massive and mixed neutrinos (3ν). This framework, that has gradually emerged from a series of beautiful experiments, represents now a "standard" paradigm of particle physics [2,3], as also highlighted by the Nobel Prize in Physics 2015 [4], that crowned decisive oscillation discoveries with natural (atmospheric and solar) neutrinos [5,6], and by the Breakthrough Prize in Fundamental Physics 2016 [7], awarded to milestone experiments using both natural and man-made (reactor and accelerator) neutrino beams [8,9].

The three-neutrino paradigm is based on the simplest assumption beyond massless neutrinos, namely, that the three known flavor states $\nu_\alpha = (\nu_e,\, \nu_\mu,\, \nu_\tau)$ are linear combinations of three states $\nu_i = (\nu_1,\, \nu_2,\, \nu_3)$ with definite masses $m_i = (m_1,\, m_2,\, m_3)$ through a unitary matrix U_{α_i}, also called the Pontecorvo–Maki–Nakagawa–Sakata [10,11] (PMNS) matrix [12]. In standard convention [3], U_{α_i} is parameterized in terms of three mixing angles $\theta_{ij} \in [0,\, \pi/2)$ and one so-called Dirac phase $\delta \in [0,\, 2\pi)$, associated to possible violations of the charge–parity (CP) symmetry in the neutrino sector,

$$U_{\alpha i} = \begin{pmatrix} c_{13}c_{12} & s_{12}c_{13} & s_{13}e^{-i\delta} \\ -s_{12}c_{23} - c_{12}s_{23}s_{13}e^{i\delta} & c_{12}c_{23} - s_{12}s_{23}s_{13}e^{i\delta} & s_{23}c_{13} \\ s_{12}s_{23} - c_{12}c_{23}s_{13}e^{i\delta} & -c_{12}s_{23} - s_{12}c_{23}s_{13}e^{i\delta} & c_{23}c_{13} \end{pmatrix} , \tag{1}$$

where $c_{ij} = \cos(\theta_{ij})$ and $s_{ij} = \sin(\theta_{ij})$.

A convention-independent measure of CP violation is given by the Jarlskog invariant [3,13]

$$J = \mathrm{Im}\left(U_{\mu 3} U_{e3}^* U_{e2} U_{\mu 2}^*\right) \tag{2}$$

$$= \frac{1}{8}\cos(\theta_{13})\sin(2\theta_{13})\sin(2\theta_{23})\sin(2\theta_{12})\sin\delta\,, \tag{3}$$

which shows at a glance that leptonic CP violation is a genuine 3ν effect [14]. In particular, $J \neq 0$ requires not only that $\delta \neq \{0,\, \pi\}$ but also that any mixing angle is nonzero ($\theta_{ij} > 0$) and that any two masses are different ($m_i \neq m_j$) – otherwise one mixing angle could be rotated away. Since the review in [1] (when only θ_{12} and θ_{23} were measured), dramatic progress has occurred concerning θ_{13} [15], starting from hints from solar, reactor and atmospheric data [16], to growing evidence from accelerator data [17–20] and finally to its discovery and precise determination via near-far detection at short-baseline reactors [21–26]. Currently, not only the J prefactor is known to be nonzero, but very interesting data from long-baseline accelerator experiments [27–30] seem to suggest a nearly maximal CP phase factor, $|\sin\delta| \sim 1$, with a significant preference for $\sin\delta < 0$ [31–35]. Another issue is the near maximality of the θ_{23} angle, $\sin^2(2\theta_{23}) \simeq 1$, that is still unresolved [27–30] in terms of a preferred octant ($\theta_{23} \leq \pi/4$ or $> \pi/4$) [36].

Concerning neutrino mass states ν_i, the standard labeling [3] $i = 1,\, 2,\, 3$ reflects the observed hierarchy of ν_e mixing with ν_i, namely, $|U_{e1}|^2 > |U_{e2}|^2 > |U_{e3}|^2$. In vacuum, oscillations of relativistic ν_i with given momentum p and energies $E(\nu_i) \simeq p + m_i^2/(2p)$ are triggered by the tiny differences $E(\nu_i) - E(\nu_j) \simeq (m_i^2 - m_j^2)/(2p)$. Using the same convention as in [1] we define two independent squared mass differences,

$$\delta m^2 = m_2^2 - m_1^2 > 0 \tag{4}$$

and

$$\Delta m^2 = m_3^2 - \frac{m_1^2 + m_2^2}{2}\,, \tag{5}$$

with two possible options for the neutrino mass spectrum ordering: either $\Delta m^2 > 0$ (normal ordering, NO) or $\Delta m^2 < 0$ (inverted ordering, IO). In matter, oscillations of ν_α are also affected by interaction energy differences $E(\nu_e) - E(\nu_{\mu,\tau}) = \sqrt{2}G_F N_e$ via the celebrated Mikheev–Smirnov–Wolfenstein (MSW) mechanism [37–39] and its variants for different profiles of the electron density $N_e(x)$ [3,40]. Oscillations in both vacuum and matter have led to measurements of δm^2 and $|\Delta m^2|$ but not yet of the sign of Δm^2 [41].

Finally, absolute neutrino masses are accessible via kinematical effects at the endpoint of β decay [42,43], approximately sensitive to the so-called effective electron neutrino mass m_β defined as [44],

$$m_\beta^2 = \sum_{i=1}^{3} |U_{ei}|^2 m_i^2 = c_{13}^2(c_{12}^2 m_1^2 + s_{12}^2 m_2^2) + s_{13}^2 m_3^2\,, \tag{6}$$

or via dynamical effects from gravitational and electroweak interactions. In particular, cosmological observations are sensitive to the sum of neutrino masses (i.e., to their "total gravitational charge") [45–48],

$$\Sigma = m_1 + m_2 + m_3\,, \tag{7}$$

and, to some extent, also to the mass spectrum ordering [49]. If neutrinos are of Majorana (instead of Dirac) type [50,51], then a rare process of two-lepton creation – the neutrinoless double beta decay ($0\nu\beta\beta$) – may occur in some nuclei [52–55], with a rate proportional to the square of the effective Majorana mass $m_{\beta\beta}$,

$$m_{\beta\beta} = \left| \sum_{i=1}^{3} U_{ei}^2 m_i \right| = \left| c_{13}^2 (c_{12}^2 m_1 + s_{12}^2 e^{i\phi_{21}} m_2) + s_{13}^2 e^{i\phi_{31}} m_3 \right| \,, \tag{8}$$

where ϕ_{ji} are additional (Majorana) CP-violating phases, here defined via the convention $U \to U \cdot \mathrm{diag}(1,\, e^{\frac{i}{2}\phi_{21}},\, e^{\frac{i}{2}(\phi_{31}+2\delta)})$ [56]. See also [57] for an interesting recent overview of formalism and conventions in neutrino physics.

Within the above 3ν framework of massive and mixed neutrinos, we currently know rather accurately five parameters, governing two oscillation frequencies and their amplitudes in different channels,

$$3\nu \text{ knowns}: \;\; \delta m^2,\; |\Delta m^2|,\; \theta_{12},\; \theta_{23},\; \theta_{13} \,, \tag{9}$$

while the following five features have not been established yet:

$$3\nu \text{ unknowns}: \;\; \delta,\;\; \mathrm{sign}(\Delta m^2),\; \mathrm{sign}(\theta_{23} - \pi/4),\; \min(m_i),\; \text{Dirac/Majorana nature} \,, \tag{10}$$

the latter option including the unknown phases ϕ_{21} and ϕ_{31} (if Majorana). In the following we shall review the status of both known and unknown features of the 3ν framework, within a global analysis of oscillation and non-oscillation data as available in April 2018. Results will be expressed in terms of standard deviations $N\sigma$ from a local or global χ^2 minimum,

$$N\sigma = \sqrt{\Delta\chi^2} \,. \tag{11}$$

This analysis follows up the previous review in this Journal [1] and updates the more recent papers in [34,35]. Interesting and independent global analyses of neutrino data have also appeared recently [31–33], and will be referred to for comparison in the following.

There are also other "unknowns" (or poorly known quantities) that affect the completion and test of the 3ν framework. On the one hand, several physics ingredients demand a deeper experimental and theoretical knowledge, at the level of neutrino production (e.g., absolute fluxes and energy spectra), evolution in time (e.g., background fermion profiles in matter, large-scale structure effects in cosmology), and detection (e.g., absolute and differential cross sections, effective weak couplings in nuclear matter). On the other hand, at any given time there are some observed phenomena that seem to go beyond the adopted "standard neutrino framework", and that might point towards novel states or interactions. A relevant example is currently provided by anomalous oscillation results suggesting mixing with light sterile neutrinos [58–61], possibly endowed with peculiar interactions to evade cosmological bounds [62–65]. An overview of these "generalized" unknown (or poorly known) aspects of neutrino physics is beyond the scope of this paper, but we shall briefly comment on some of them while discussing the "proper" 3ν knowns and unknowns in Eqs. (9) and (10), especially to highlight 3ν aspects which deserve further attention.

The paper is organized as follows. In Section 2 we discuss the methodology and the updates used to analyze solar, long-baseline reactor, long-baseline accelerator, short-baseline reactor, and atmospheric ν oscillation data. With respect to [1] and also to more recent analyses [34,35] we now use official χ^2 maps provided by experimental collaborations for some datasets (including short-baseline reactor and atmospheric neutrinos) that are difficult to reproduce by external users, and discuss pros and cons of this choice. In Section 3 we discuss the global fit results in terms of single (known and unknown) oscillation parameters. We find persisting hints in favor of $\sin\delta < 0$ and significant indications in favor of normal spectrum ordering, at the level of $N\sigma \simeq 3$. Concerning θ_{23}, we find a rather restricted range near maximal mixing, with a slight preference for the second octant. In Section 4 we explore in further detail such results in terms of covariances between pairs of parameters, which highlight the interplay among different datasets. In Section 5 we combine oscillation data with nonoscillation constraints from cosmology and neutrinoless double beta decay, in order to derive upper bounds on absolute neutrino masses, which are of interest also for neutrino mass searches with beta decay. Our summary and conclusions are reported in Section 6.

A final remark is in order. As in [1], we aim at presenting a state-of-the-art global analysis of 3ν knowns and unknowns, but we do not aim at being bibliographically complete. A useful starting point for orientation in the vast neutrino literature is [66]. Recent books with useful references on various aspects of our current understanding (and future prospects) of the neutrino mass-mixing phenomenology and its relation with astroparticle physics and cosmology include [67–77]. With respect to [1], we do not insist anymore on statistical aspects that have now become standard tools in the field (such as details of the pull method [78] and of its various applications in χ^2 analyses), but prefer to comment on future challenges that are emerging from analyses of current and prospective data.

2. Analysis of oscillation data: Methodology and updates

In the review [1], it was found that the mixing angle θ_{13} was compatible with zero at $\sim 1\sigma$, although its best-fit value ($\sin^2\theta_{13} \sim 10^{-2}$) was already in the right ballpark of later discoveries. At that time, under the assumption $\theta_{13} \simeq 0$ suggested by the CHOOZ null results [15], it was methodologically convenient – before performing a global fit – to group oscillation

data in two classes: solar plus long-baseline reactor data, mainly sensitive to $(\delta m^2,\ \theta_{12})$, and atmospheric and long-baseline accelerator data, mainly sensitive to $(\Delta m^2,\ \theta_{23})$ [1].

Subsequently, the growing indications in favor of $\sin^2\theta_{13} \sim 0.01$–$0.02$ [16] and its experimental discoveries via $\nu_e \to \nu_e$ flavor disappearance at reactors [8] and $\nu_\mu \to \nu_e$ appearance at accelerators [9], have opened a portal to genuine 3ν effects at subleading level [25,79], such as possible signs of CP violation driven by δ [29] and, more recently, to possible indications about the mass ordering [80]; see also [31–35]. In this context, a different grouping of data was proposed in [25], in order to show more clearly the progressive impact of different datasets on both known and unknown parameters. The same methodology is also adopted herein, being supported by additional reasons that we now discuss.

The starting point is provided by solar and long-baseline reactor data, that probe the $\nu_e \to \nu_e$ flavor disappearance channel via oscillations driven by the $(\delta m^2, \theta_{12}, \theta_{13})$ parameters. These data provide precise measurements of $(\delta m^2, \theta_{12})$ and a rough measurement of $\theta_{13} > 0$ at the $\sim 2\sigma$ level. On the other hand, long-baseline accelerator data probe both the $\nu_\mu \to \nu_\mu$ disappearance and the $\nu_\mu \to \nu_e$ appearance channel via oscillations driven mainly by the $(\Delta m^2,\ \theta_{23},\ \theta_{13})$ parameters, but they are also sensitive to subleading effects driven by $(\delta m^2, \theta_{12})$, as well as by δ and $\mathrm{sign}(\Delta m^2)$. The interesting new fact is that such data provide, in combination, not only a good measurement for each of the five parameters in Eq. (9), but also precious hints in favor of $\sin\delta \neq 0$ (i.e., CP violation) and of $\mathrm{sign}(\Delta m^2) = +1$ (i.e., normal ordering), as shown in Section 3. It turns out that these hints are enhanced by adding first short-baseline reactor data, mainly sensitive to $(\Delta m^2,\ \theta_{13})$, and then atmospheric neutrino data, sensitive in different ways to all the oscillation parameters via disappearance and appearance channels. Therefore, this methodological approach allows to gauge how the current indications about neutrino CP violation and mass spectrum ordering are progressively enhanced, by using increasingly rich datasets in the global analysis.

In the following, we discuss relevant updates for the various datasets, in the same order as suggested by the above methodology. The reader not interested in technical details may skip the rest of this Section and jump to the results in Section 3.

2.1. Solar and long-baseline reactor (KamLAND) neutrinos

Concerning solar neutrinos, with respect to the recent analyses in [34,35] we now include the latest low-energy Borexino data [81–83] and Super-Kamiokande-IV data (day and night) [84]. We have revisited our analysis of three-phase data from the Sudbury Neutrino Observatory (SNO), obtaining results in closer agreement with the official SNO ones reported in [85] for the mass-mixing parameter region allowed at large mixing angle (LMA). Inputs from radiochemical experiments remain as reported in [86] (Homestake) for Chlorine and in [87,88] (GALLEX-GNO + SAGE) for Gallium.

We adopt reference solar neutrino fluxes from the standard solar model named B16-GS98 in [89], which ameliorates the tension with helioseismological data. Systematic nuisance uncertainties are taken from [89] and, when needed, they are supplemented by related information from [90]. The ^{8}B neutrino spectrum and its uncertainties are taken from [91].

The Gallium (Ga) neutrino absorption cross-section $\sigma_{\mathrm{Ga}}(E_\nu)$ and its uncertainties have been updated according to the recent experimental results and estimates in [92] (see also [93]). The results of [92] lead to a reduction of the unoscillated solar neutrino rate in Ga by $\sim$ 6 SNU (solar neutrino units [94]) for our adopted reference fluxes [89] (the reduction by $\sim$ 10 SNU quoted in [92] being due to somewhat different fluxes). The generic impact of Ga cross-section variations was discussed in [95], where it was shown that, in combination with SNO, a reduction of σ_{Ga} tends to slightly decrease θ_{12} and increase δm^2 for nonzero θ_{13} (see Figs. 8 and 9 in [95]). These qualitative expectations are confirmed in our analysis.

Concerning long-baseline reactor neutrino oscillations in the KamLAND (KL) experiment [96], we adopt the same reanalysis of the 2011 KL dataset [97] performed in [34], which included in the reactor spectra [98,99] the "bump" feature recently observed around energies $E_\nu \sim$ 5–7 MeV [100–103], which is still poorly understood [104–107]. Such a reanalysis has led to a tiny reduction of the $(\delta m^2,\ \theta_{12})$ best-fit values in KL [34], see also [108]. In this context, an official KL analysis update (including current information on reactor spectra and uncertainties) would be beneficial.

As in [34], we cannot use the latest published KL data [96] herein. They are presented in a peculiar format (consisting of three subsets with correlated systematics) that prevents a proper detailed analysis outside the collaboration. This drawback is representative of a more general situation that is becoming increasingly common in neutrino physics – as also discussed later in this review – and that parallels other fields of particle physics involving multiple and complex experimental inputs, such as global analyses of electroweak data [109,110] and of parton distribution functions [110–113]. Indeed, as the experiments become more refined and collect higher statistics with trickier dependence on systematics, the data analysis also gets more complicated, eventually becoming nearly prohibitive outside the collaborations. However, external users may need to perform their own data fits for diverse purposes, e.g., for global analyses as in this work, or for phenomenological tests of specific theoretical models, or for sensitivity estimates of prospective signals. One can then adopt different approaches to such situation, with various pros and cons, including: (a) continue to analyze (some) available data within reasonable approximations or well-defined restrictions, but with increasing awareness of the inherent uncertainties; (b) discard raw data in favor of officially "processed" results (e.g., via χ^2 maps or dedicated software tools, if any) that, however, may prevent testing analysis details or variants; (c) just give up on some data (sub)sets. Given the complex issues involved, one should maintain an open attitude about different choices (that may be dictated by objective difficulties as well as by subjective assessments), and foster a continuous dialogue between internal collaboration teams and external researchers, so as to use the precious experimental data in the best possible way to advance neutrino phenomenology and theory.

We conclude by reminding that the 3ν survival probability relevant for solar and KamLAND neutrino data can be cast in the form [3,108]:

$$P_{3\nu}(\nu_e \to \nu_e) \simeq \cos^4\theta_{13}\, P_{2\nu}(\nu_e \to \nu_e) + \sin^4\,\theta_{13}\,, \tag{12}$$

where $P_{2\nu}$ corresponds to the 2ν probability for $\theta_{13} = 0$, which depends on the $(\delta m^2,\, \theta_{12})$ parameters only. For solar neutrinos, one should replace θ_{13} with its effective value in matter $\tilde{\theta}_{13}$, which carries a slight dependence on Δm^2 and on the mass ordering [1,114].

2.2. Long-baseline accelerator neutrinos

At the time of the previous review [1] on this Journal, long-baseline (LBL) accelerator searches for $\nu_\mu \to \nu_\mu$ disappearance had been performed only by the KEK-to-Kamioka (K2K) experiment [115,116], later followed by the Main Injector Neutrino Oscillation Search (MINOS) experiment [117] that also started to search for $\nu_\mu \to \nu_e$ appearance [118]. The successful search for $\nu_\mu \to \nu_\tau$ appearance in the Oscillation Project with Emulsion-tRacking Apparatus (OPERA) [119] has provided further confidence in the 3ν framework, although the data in this channel do not significantly constrain the 3ν oscillation parameters.

Two main experiments currently drive the search for both $\nu_\mu \to \nu_\mu$ and $\nu_\mu \to \nu_e$ oscillations with LBL accelerator neutrino and antineutrino beams, namely, the Tokai-to-Kamioka (T2K) experiment in Japan [29,120] and the Neutrino at main injector Off-axis ν_e Appearance experiment in the U.S. [30]. A powerful software, the General Long Baseline Experiment Simulator (GLoBES) [121,122] has also become publicly available to analyze this class of experiments, including a full-fledged treatment of statistical and systematic uncertainties. Previous analyses that included T2K and NOvA results via adapted versions of GLoBES have been discussed in [34,35].

Very recently, updated disappearance and appearance data have been presented for both T2K [123] and NOvA [124]. For T2K [123], disappearance data include 240 ν_μ events and 68 $\overline{\nu}_\mu$ events in the charged-current quasi-elastic (CCQE) class, divided into 27 equally-spaced bins in the reconstructed energy range $[0.2,\ 2.9]$ GeV, plus a 28th bin (4 GeV wide) for higher energies. Appearance data include 74 CCQE ν_e, 7 CCQE $\overline{\nu}_e$ and 15 CC1π (one pion) e-like events, divided into 9 equally-spaced bins in the interval $[0.125,\ 1.25]$ GeV. Background events are taken from [123] and assumed to be oscillation-independent. In our analysis, software-generated disappearance and appearance spectra are calibrated so as to reasonably reproduce the official spectra at the oscillation best-fit point, which require $\sim$ 15% energy resolution smearing. Agreement with official parameter bounds is also optimized by slightly tuning nuisance parameters, including the normalization uncertainties that we set at the level of 7% (CCQE ν_e and $\overline{\nu}_e$), 9% (background ν_e and $\overline{\nu}_e$), 7% (CCQE ν_μ and $\overline{\nu}_\mu$ background and signal events), and 20% (CC1π) A likelihood function L including Poisson statistics [125] is then constructed and converted into $\chi^2 = -2\log(L)$.

For NOvA [124], disappearance data include 126 ν_μ events, divided into 4 subsets called "quantiles", each of them corresponding to different energy resolutions (6, 8, 10 and 12%) and to 18 bins with different width. Appearance data include 57 ν_e events divided into 6 equally-spaced bins in the interval $[1,\ 4]$ GeV; we do not consider a further separation into three subclasses with different values of the particle identification (PID) parameter [124]. Also included are 9 so-called peripheral ν_e events grouped in a single bin. Further details on NOvA data can be found in [126]. As for T2K, also NOvA backgrounds are assumed to be oscillation-independent, oscillated spectra are tuned at best fit, and nuisance parameters are slightly adjusted. In particular, we assume 10% normalization error for ν_e background and signal events, and 20% and 5% errors for the normalization and calibration of ν_μ events, respectively. A Poissonian χ^2 is then constructed.

We obtain very good agreement with all the oscillation parameter constraints shown in [123] for T2K and in [124] for NOvA, under the same assumptions used therein about θ_{13} (usually restricted around $\sin^2\theta_{13} \simeq 0.02$). We emphasize that no restrictive assumption is made when the T2K and NOvA data are included in the global analysis, all the parameters being left free. We also remark that T2K and NOvA appearance data are now accurate enough to require analyses in terms of binned spectra rather than of total rates, the latter being less constraining: this represents tremendous progress in the field. Finally, it should be noticed that the two collaborations are working towards the formation of a joint analysis group producing a full T2K+NOvA combined analysis by 2021 [127].

We conclude by reminding that the 3ν appearance probability of accelerator neutrinos (traveling along a baseline x in constant N_e) can be approximately cast in the form (in natural units) [128,129]:

$$\begin{aligned} P(\nu_\mu \to \nu_e) \simeq\ & \sin^2\theta_{23}\sin^2 2\theta_{13}\left(\frac{\Delta m^2}{A-\Delta m^2}\right)^2 \sin^2\left(\frac{A-\Delta m^2}{4E}x\right) \\ & + \sin 2\theta_{23}\sin 2\theta_{13}\sin 2\theta_{12}\left(\frac{\delta m^2}{A}\right)\left(\frac{\Delta m^2}{A-\Delta m^2}\right)\sin\left(\frac{A}{4E}x\right)\sin\left(\frac{A-\Delta m^2}{4E}x\right)\cos\left(\frac{\Delta m^2}{4E}x\right)\cos\delta \\ & - \sin 2\theta_{23}\sin 2\theta_{13}\sin 2\theta_{12}\left(\frac{\delta m^2}{A}\right)\left(\frac{\Delta m^2}{A-\Delta m^2}\right)\sin\left(\frac{A}{4E}x\right)\sin\left(\frac{A-\Delta m^2}{4E}x\right)\sin\left(\frac{\Delta m^2}{4E}x\right)\sin\delta \\ & + \cos^2\theta_{13}\sin^2 2\theta_{12}\left(\frac{\delta m^2}{A}\right)^2 \sin^2\left(\frac{A}{4E}x\right)\,, \end{aligned} \tag{13}$$

where $A = 2\sqrt{2}G_F N_e E$ governs matter effects, with $A \to -A$ and $\delta \to -\delta$ for $\nu \to \overline{\nu}$, and $\Delta m^2 \to -\Delta m^2$ for normal to inverted ordering. At typical NOvA energies ($E \sim 2$ GeV) it is $|A/\Delta m^2| \sim 0.2$, and significant matter effects can build up along the baseline $x = 810$ km. At the lower T2K energies, the ratio $|A/\Delta m^2|$ is a factor 3–4 smaller, and the baseline ($x = 295$ km) is also smaller, so that oscillations are almost vacuum-like. See also [130–134] for recent analytical studies of 3ν probabilities at accelerator baselines and energies. Note that the above form for $P_{\mu e}$, despite being useful for later discussions, is not used in our analysis, which is based on full 3ν numerical probabilities in matter (for both appearance and disappearance channels) without any approximation.

2.3. Short-baseline reactor neutrinos

At the time of [1], short-baseline reactor neutrino results [15] were compatible with null oscillations within statistical and systematic errors. The development of the near-far detection technique [135] and the construction of massive detectors allowed to reduce the uncertainties and to discover θ_{13}, currently measured by three experiments: Daya Bay [22,103,136], RENO [23,101,137] and Double Chooz [21,102,138]; see [139–141] for recent reviews. Detailed spectral information actually allows to determine joint bounds on $(\Delta m^2,\ \theta_{13})$, as demonstrated by RENO [142] and Daya Bay [136], the latter setting bounds on Δm^2 competitive with those from LBL accelerator data [141]. These results represent a major success of reactor neutrino physics.

Among reactor experiments, Daya Bay [136] dominates current bounds on $(\Delta m^2,\ \theta_{13})$, the corresponding uncertainties being a factor ~ 2.5 smaller than in RENO [137,142] and significantly smaller than in Double Chooz [138] (see also [141]). Recent analyses have shown that the reactor data combination only leads to fractional differences (well below 1σ) in comparison with bounds from Daya Bay data alone [31,33].

Systematic errors are already comparable to statistical ones in both Daya Bay and RENO, and some systematics are shared by all reactor experiments including Double Chooz. Therefore, a proper combination should take into account a common set of nuisance parameters affecting the three experiments at the same time, within a unified analysis framework. A joint analysis might possibly clarify the apparent preference of Double Chooz for higher values of θ_{13} [141] as compared with Daya Bay and RENO. Work is in progress towards this (technically difficult but scientifically worthwhile) joint analysis, as testified by dedicated meetings [143,144] and ongoing common activities mentioned, e.g., in [145–147]. For the purposes of this work, lacking a full understanding of common systematics, we choose to limit ourselves to using the official χ^2 map from Daya Bay alone in the global analysis. Such a Daya Bay map is provided in terms of $\chi^2 = \chi^2(\Delta m^2_{ee},\ \sin^2\theta_{13})$ [148], where the effective parameter Δm^2_{ee} [149] can be converted into Δm^2 via the relation [150,151]

$$\Delta m^2_{ee} = |\Delta m^2| \pm (c^2_{12} - s^2_{12})\delta m^2/2\ , \tag{14}$$

where the upper (lower) sign refers to NO (IO). A proper combination of data and correlated uncertainties from all three reactor experiments is left as a future opportunity.

2.4. Atmospheric neutrinos

Atmospheric neutrinos represent a very important and rich source of information on neutrino oscillations, culminating in the discovery of $\nu_\mu \to \nu_\mu$ disappearance driven by $(\Delta m^2,\ \theta_{23})$ in 1998 [152,153]. The wide range of energies and baselines probed by atmospheric neutrinos and antineutrinos of both muon and electron flavors, makes them sensitive to interesting multi-layer matter effects [154–157] and to all the oscillation parameters in the 3ν framework [158–160], although only the dominant ones $(\Delta m^2,\ \theta_{23})$ have been really measured (with stringent upper and lower bounds) within this data sample so far [161].

In general, the event rate R_β for lepton-like events of flavor $\beta = e,\ \mu$ induced by atmospheric neutrinos of the same (β) or different (α) flavor must be estimated through multi-dimensional integrals of the form [162–165]

$$R_\beta = \int (\Phi_\beta P_{\beta\beta} + \Phi_\alpha P_{\alpha\beta}) \otimes \sigma_\beta \otimes r_\beta \otimes \varepsilon_\beta\ , \tag{15}$$

where Φ represents the initial neutrino fluxes, P the oscillation probability, σ the cross section, and r and ε the detection resolution for the final-state lepton, while $\otimes$ generically denotes convolution. The rates R_β are usually subdivided according to specific event topologies to specific ranges in observed energy and angular (bins). Finite energy and direction resolutions smear out considerably the information in P over binned spectra. All these ingredients come with their own uncertainties, which need to be estimated and propagated to the various spectra, often inducing sample-to-sample and bin-to-bin correlations of systematics [164,166]. See also [167,168] for statistical issues in the analysis of prospective data from future large-volume atmospheric neutrino detectors. The whole analysis is quite sophisticated and is becoming increasingly difficult – if not impossible – to be constructed outside the experimental collaborations themselves.

For instance, the latest Super-Kamiokande (SK) atmospheric data samples include as many as 520 bins in energy–angle and 155 systematic parameters [80], whose complete analysis vastly exceeds the capabilities of any external user. In particular, recent techniques for the statistical separation of ν_e and $\overline{\nu}_e$ event in dedicated samples [80], which provide enhanced sensitivity to matter effects, neutrino CP violation and mass ordering, have been implemented via neural-network simulations of the detection process [169]. Another issue is represented by incomplete (or missing) public information. As an

example, the IceCube DeepCore (IC-DC) atmospheric data release in [170] was accompanied by a public analysis toolkit [171], but such tools have not (yet) been provided for the latest data release in [172], preventing a direct use by external users. This drawback has been recently compensated by the availability of IC-DC χ^2 maps [173] derived from the official oscillation analysis in [172].

There may be different approaches to these issues, especially concerning the vast and complex SK dataset. One may limit the analysis to those subsets of SK atmospheric data which can be reliably reproduced outside the collaborations, as it was attempted in most global analyses so far, including, e.g., [1,25,26,34,164,174]. Alternatively, one may use official χ^2 maps from SK if available, as advocated in [24,33] that included the results in [175,176]. Note, however, that such maps were obtained in the one-dominant mass-scale approximation ($\delta m^2 = 0$) [175,176] and thus, by construction, they are insensitive to several subleading 3ν effects, including CP violation. Eventually – and more radically – one may just "give up" on the analysis of SK atmospheric data and exclude them altogether, as recently advocated in [31,32].

In this work, we prefer to abandon our own analysis of SK atmospheric data, improved over the last twenty years [35,163]. We feel that our attempts to analyze these data are no longer competitive with the official SK ones, as unavoidable approximations and data selections might bias or hinder the emergence of small, subleading effects. However, it makes sense to keep such data in the global analysis, since the full SK atmospheric sample clearly shows an increasing sensitivity to several 3ν "unknowns" [80], especially in combination with reactor and accelerator data. We thus adopt the official SK χ^2 maps derived in [80] through a full 3ν analysis of atmospheric data (without external constraints from reactor or accelerator experiments), which recently became publicly available [177]. These SK χ^2 maps are provided for both NO and IO in terms of four relevant parameters (Δm^2, θ_{23}, θ_{13}, δ), with (δm^2, θ_{12}) fixed at best fit. We also adopt the maps provided by IC-DC for their latest datasets [172,173] in terms of the two dominant parameters (Δm^2, θ_{23}) for both NO and IO, with (δm^2, θ_{12}) fixed at best fit, the dependence on θ_{13} and δ being negligible at the current level of accuracy in IC-DC data [178].

We conclude this section by discussing the context and implications of this choice. Atmospheric neutrinos provide free beams with wide dynamical range in energy and pathlength, which will always provide a vast amount of interesting data (signal or background) in underground detectors. In particular, they still contain very rich oscillation physics to be explored, especially in terms of subleading 3ν effects [159,179,180] that, however, can emerge only through increasingly sophisticated analyses. Probably only the experimental collaboration are (and will be) able to study their own atmospheric data at such a refined level. This transition should be accompanied by a continuous dialogue with the scientific community, in order to make progress on several "unknowns" or poorly known quantities that may hide the relevant atmospheric neutrino physics, including e.g., the systematics of cosmic ray fluxes, atmosphere parameters, cascade evolution models, three-dimensional effects, event spectral shapes, resolution tails, effective volume estimates, detection cross sections, etc. The renewed interest in these issues is testified by recent dedicated atmospheric ν workshops [181,182], in addition to traditional series with broader scope [183,184]. Such topics will become even more crucial in the future, to make the best possible use of high-statistics data coming from new-generation projects [185] such as PINGU [186,187], KM3NeT-ORCA [188], Hyper-Kamiokande [189] and INO [190].

In summary, we continue to perform an independent analysis of solar and KamLAND data, as well as of long-baseline accelerator neutrino data (with updated results from T2K [123] and NOvA [124]), whose combination provides bounds on the whole set of 3ν oscillation parameters (δm^2, Δm^2, θ_{12}, θ_{13}, θ_{23}, δ). For the first time, we use processed results rather than original data for the other datasets. In particular, we include short-baseline reactor data constraints via the official Daya Bay map $\chi^2(\Delta m^2, \theta_{13})$ [148], and finally atmospheric neutrino data via the official SK map $\chi^2(\Delta m^2, \theta_{23}, \theta_{13}, \delta)$ [177] and the IC-DC map $\chi^2(\Delta m^2, \theta_{23})$ [173]. We have argued that using (some) processed results from experimental collaborations is becoming unavoidable in global analyses, although this transition should be accompanied by critical discussions and further advances in several related subfields. We have limited ourselves to the 3ν paradigm, but the same arguments apply to the analysis of possible subleading effects coming from extended frameworks with new neutrino states or interactions.

3. Results on single oscillation parameters

In this section we present the bounds on known and unknown 3ν oscillation parameters, coming from the datasets discussed in the previous section. Bounds are shown in terms of single parameters, all the others being marginalized away. The discussion of some detailed features, that involve the interplay between different parameters (covariances) is postponed to Section 4. The main new result is the emerging indication in favor of NO at $\sim 3\sigma$ in the global analysis, with coherent contributions from all datasets. We also briefly compare our results with those obtained in other recent analyses [31–33] under homogeneous assumptions as far as possible.

3.1. Synopsis with increasingly large datasets

Analysis of long-baseline accelerator, solar and KamLAND data. Fig. 1 shows the bounds on single oscillation parameters, in terms of standard deviations $N\sigma$ from the best fit, for both NO (solid blue lines) and IO (dashed red lines), with separate χ^2 minimization for the two mass orderings. Symmetric and linear curves would correspond to Gaussian errors, a situation approximately realized for the parameters δm^2, θ_{12} and Δm^2. Strong upper and lower bounds are placed on the Δm^2, θ_{23} and θ_{13} parameters. Thus, the combination of long-baseline accelerator, solar and KamLAND data provides, by itself, a measurement of the known oscillation parameters. In addition, interesting hints emerge on the unknown ones.

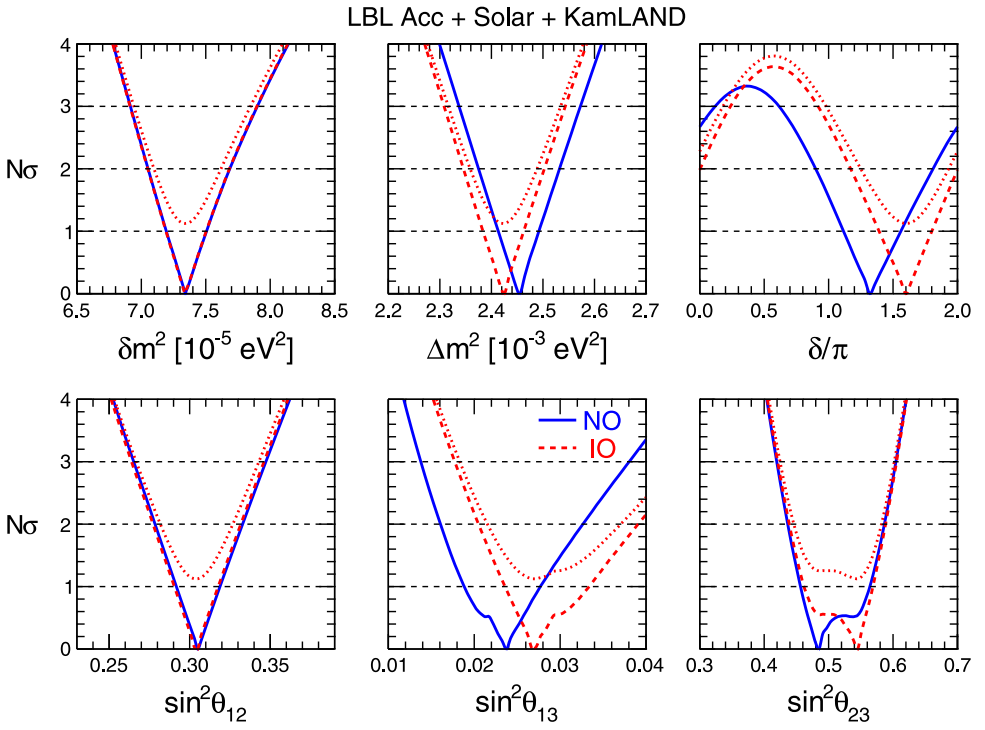

Fig. 1. Analysis of long-baseline accelerator, solar and KamLAND data. Bounds on the mass-mixing parameters are given in terms of standard deviations $N\sigma = \sqrt{\chi^2 - \chi^2_{\rm min}}$ for both normal ordering (NO, solid blue lines) and inverted ordering (IO, dashed red lines), taken separately. For IO, bounds are also shown with respect to the absolute $\chi^2_{\rm min}$ for NO (dotted red curves). The IO is slightly disfavored, at the level of $N\sigma \simeq 1.1$.

Concerning the phase δ, the CP-conserving values $\delta = \{0,\ \pi\}$ are allowed at $\sim 2\sigma$ or less in both NO and IO. However, there is a clear preference for values around $\delta \sim 3\pi/2$, i.e. for nearly maximal CP violation with $\sin\delta \sim -1$, while values near the opposite case with $\sin\delta \sim +1$ are disfavored at more than 3σ. Concerning the octant of θ_{23}, there is a slight preference for $\theta_{23} < \pi/4$ in NO and $\theta_{23} > \pi/4$ in IO, but both octants are allowed at 1σ.

Concerning the mass ordering, Fig. 1 shows that the bounds on both δm^2 and θ_{12} (dominated by solar+KL data) are almost completely insensitive to it. On the contrary, some differences are found between NO and IO for the best-fit values and allowed ranges of the parameters ($\Delta m^2,\ \theta_{23},\ \theta_{13},\ \delta$), that are constrained by long-baseline accelerator data. In particular, there is a preference for higher θ_{13} in IO. We also find an overall difference between the two χ^2 minima in NO and IO, that amounts to

$$\chi^2_{\rm min}({\rm IO}) - \chi^2_{\rm min}({\rm NO}) = 1.3\ \ ({\rm LBL\ acc.} + {\rm solar} + {\rm KL\ data})\,, \tag{16}$$

corresponding to a slight preference for NO at the level of $N\sigma \simeq 1.1$.

We thus show in Fig. 1 the parameter bounds for IO in terms of $N\sigma$, also by taking into account the absolute minimum in NO (dotted red lines). For any parameter in Fig. 1, marginalization over the (unknown) hierarchy information would correspond to taking the union of the allowed ranges at some $N\sigma$ for NO (blue solid curves) and for the displaced IO ones (dotted red curves).

The $\Delta\chi^2$ difference in Eq. (16) is almost entirely driven by the recent T2K and NOvA data. Older K2K and MINOS data are less relevant, and actually their removal would lead to a slightly higher preference for NO (not shown). Further T2K and NOvA results, possibly combined by the Collaborations themselves [127], will be crucial to test the current trend favoring NO over IO in this data sample.

Adding short-baseline reactor data. Fig. 2 is analogous to Fig. 1, but includes short-baseline reactor constraints as described in Section 2. With respect to Fig. 1, the allowed range for θ_{13} is strongly reduced, with nearly linear and symmetric bounds for both NO and IO. Also the allowed range for Δm^2 is noticeably reduced, showing that reactor neutrinos are already competitive with long-baseline accelerators in determining the largest oscillation frequency driven by Δm^2. Both parameters ($\Delta m^2,\ \theta_{13}$) depend much less on the mass ordering than in Fig. 1.

Concerning the unknown parameters, the octant ambiguity of θ_{23} remains unresolved, but there is a mild overall preference for $\theta_{23} > \pi/4$, more pronounced for IO. The indications in favor of nearly maximal CP violation are instead

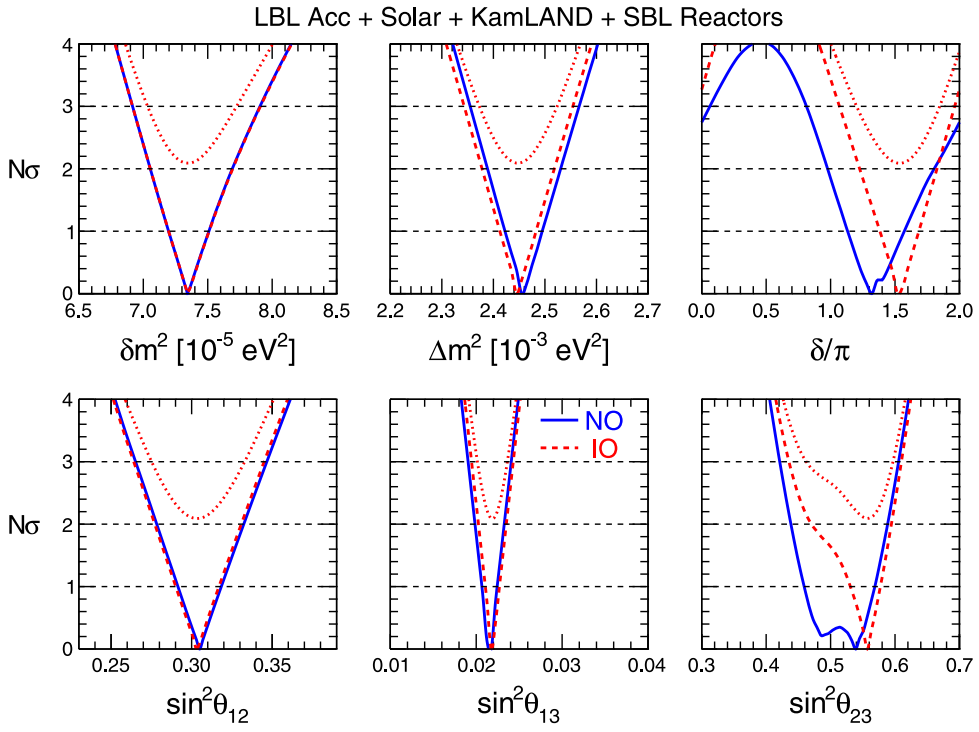

Fig. 2. Analysis of long-baseline accelerator, solar and KamLAND data, and short-baseline reactor data. Line styles and colors are as in Fig. 1.

strengthened, and the CP-conserving values of δ are now disfavored at the level of $> 1.8\sigma$ in NO and $> 3\sigma$ in IO. Significant ranges for δ are excluded at $> 3\sigma$ in both NO and IO. The preference for NO is also corroborated, and amounts to

$$\chi^2_{\rm min}({\rm IO}) - \chi^2_{\rm min}({\rm NO}) = 4.4 \ \ ({\rm LBL\ acc.} + {\rm solar} + {\rm KL} + {\rm SBL\ reac.\ data})\,, \tag{17}$$

corresponding to an interesting confidence level $N\sigma \simeq 2.1$. As discussed in more detail in Section 4, the above result stems mainly from a slight θ_{13} tension in IO between reactor and accelerator data, the latter preferring higher values of θ_{13} than the former.

Adding atmospheric neutrinos: Global analysis of all oscillation data. Fig. 3 is analogous to Fig. 2, but includes atmospheric neutrino constraints as described in Section 2. With respect to Fig. 2, the main differences concern the unknown oscillation parameters. There is a more pronounced preference for $\theta_{23} > \pi/4$, although both octants are allowed at $< 2\sigma$. The preference for CP violation with $\sin\delta < 0$ is confirmed, while CP conservation is disfavored at $> 1.9\sigma$ for NO and $> 3.5\sigma$ for IO. Remarkably, the sensitivity of atmospheric data to the mass ordering is also consistent with the hints from previous datasets and leads to

$$\chi^2_{\rm min}({\rm IO}) - \chi^2_{\rm min}({\rm NO}) = 9.5 \ \ ({\rm all\ oscillation\ data})\,, \tag{18}$$

corresponding to a statistically significant confidence level $N\sigma \simeq 3.1$. The increase from Eq. (17) to Eq. (18) is mainly due to SK atmospheric data [80], but there is also a synergic contribution (by about one unit of $\Delta\chi^2$) from IC-DC data, that will be discussed in Section 4.

3.2. Summary and discussion of results

The preference for NO at the level of $\Delta\chi^2 \sim 9$ in Eq. (18) represents an interesting result of our work. This indication emerges consistently for increasingly rich datasets, as shown by the progression in Eqs. (16)–(18), and thus deserves attention. Taken at face value, a 3σ rejection of IO would imply that the only relevant scenario is NO, together with its parameter ranges (see Fig. 3).

However, caution should be exercised at this stage, since the value $\Delta\chi^2 \sim 9$ derives from two main contributions of comparable size $\Delta\chi^2 \simeq 4$–5 (corresponding to $\sim 2\sigma$) but with rather different origin. One contribution [Eq. (17)] comes basically from long-baseline accelerator data and their interplay with short-baseline reactor data, where mass-ordering effects can be understood with relatively simple arguments in terms of θ_{13} (see next Section). The other incremental

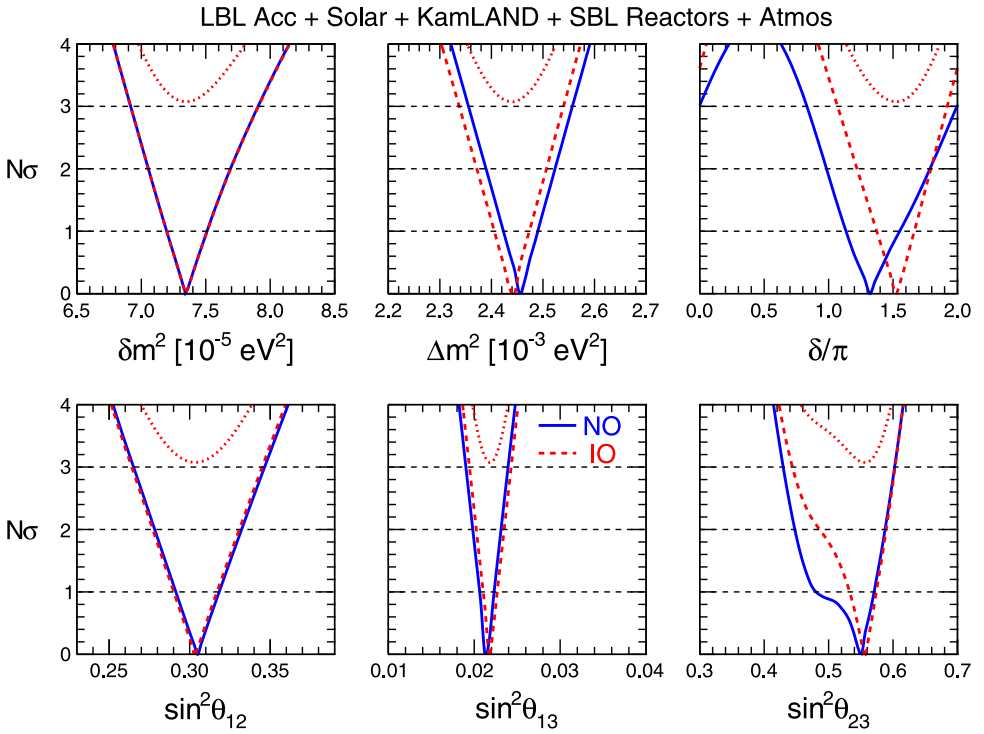

Fig. 3. Global analysis of oscillation data from long-baseline accelerator, solar and KamLAND, short-baseline reactor, and atmospheric neutrino experiments. Line styles and colors are as in Fig. 1.

contribution [from Eqs. (17) to (18)] comes basically from atmospheric data, where mass-ordering effects are not apparent "at a glance", but are indirect and largely smeared over various energy–angle spectra [80]. A wise attitude is to wait for further data from all the running experiments which, in the next few years, can reveal if these two hints at $\sim 2\sigma$ level will fluctuate down, or will consistently grow and confirm the preference for NO at a cumulative level $> 3\sigma$. On a longer time frame, discovery-level tests of the mass spectrum ordering will be provided by next-generation projects [41], not only with large-volume atmospheric neutrinos [187–190] but also with medium-baseline reactors [191] such as JUNO [192] and new long-baseline accelerator facilities such as T2HK [193], DUNE [194] and ESSnuSB [195]. Finally, for discrete hypotheses like NO versus IO, the statistical interpretation of $\Delta\chi^2$ in terms of $N\sigma$ remains effectively applicable, but must be taken with a grain of salt [196].

In the following, we shall thus conservatively report the allowed ranges for NO and IO as if they were two separate and equally acceptable cases, without including the large χ^2 difference of IO with respect to the absolute minimum in NO [Eq. (18)]. Marginalization over "any ordering" (as performed, e.g., in [31,32,35]) is not considered herein.

Table 1 reports in numerical form what is shown in Fig. 3 for NO and IO separately, in terms of best-fit values and allowed ranges at $N\sigma = 1,\ 2,\ 3$ level. The last column reports the fractional "1σ" accuracy, defined as 1/6 of the 3σ range, divided by the best-fit value. From top to bottom, the rows of Table 1 provide information on both known and unknown 3ν parameters. The two known parameters δm^2 and $\sin^2\theta_{12}$, dominated by solar and KamLAND data, are basically the same in NO and IO, up to tiny variations discussed later in Section 4. They are determined with an accuracy of 2.2 and 4.4%, respectively. The value of $\sin^2\theta_{13}$, dominated by reactor data, is also determined with a very good accuracy of $\sim$ 3.8%. The best known parameter is $|\Delta m^2|$, which is currently determined with a remarkably small uncertainty of 1.4% in each of the two mass orderings, as a result of consistent and comparable constraints from long-baseline accelerator, reactor and atmospheric neutrino data.

The least accurate among the known oscillation parameters in Table 1 is $\sin^2\theta_{23}$, with an uncertainty of $\sim$ 5%. As compared with previous analyses [34,35], the θ_{23} uncertainty is smaller, as a result of a better convergence of recent NOvA data [124] towards quasi-maximal mixing, in agreement with T2K and atmospheric data. Maximal mixing is allowed at $< 2\sigma$ in both NO and IO, and thus the octant degeneracy remains unsolved. Concerning δ, Fig. 3 shows that there is a single 3σ range around its best fit, with relatively linear and symmetric errors, in both NO and IO. Nonlinear errors, also due to the cyclic nature of δ, emerge only at a level $> 3\sigma$ in NO and $> 4\sigma$ in IO. Within $< 3\sigma$, one can tentatively say that δ is "determined" with an accuracy of $\sim$ 15% ($\sim$ 9%) in NO (IO), as reported in Table 1.

Summarizing, the "known" oscillation parameters δm^2, Δm^2, $\sin^2\theta_{12}$, $\sin^2\theta_{13}$ and $\sin^2\theta_{23}$ are currently measured at the few % level. Concerning the "unknown" oscillation parameters, interesting indications emerge in favor of NO at a global 3σ level. At the same level one can also determine upper and lower limits for the phase δ, with preference for nearly maximal

Table 1
Best fit values and allowed ranges at $N\sigma = 1,\ 2,\ 3$ for the 3ν oscillation parameters, in either NO or IO. The latter column shows the formal "1σ accuracy" for each parameter, defined as 1/6 of the 3σ range divided by the best-fit value (in percent).

Parameter	Ordering	Best fit	1σ range	2σ range	3σ range	"1σ" (%)
$\delta m^2/10^{-5}$ eV^2	NO	7.34	7.20–7.51	7.05–7.69	6.92–7.91	2.2
	IO	7.34	7.20–7.51	7.05–7.69	6.92–7.91	2.2
$\sin^2\theta_{12}$	NO	3.04	2.91–3.18	2.78–3.32	2.65–3.46	4.4
	IO	3.03	2.90–3.17	2.77–3.31	2.64–3.45	4.4
$\sin^2\theta_{13}/10^{-2}$	NO	2.14	2.07–2.23	1.98–2.31	1.90–2.39	3.8
	IO	2.18	2.11–2.26	2.02–2.35	1.95–2.43	3.7
$\lvert\Delta m^2\rvert/10^{-3}$ eV^2	NO	2.455	2.423–2.490	2.390–2.523	2.355–2.557	1.4
	IO	2.441	2.406–2.474	2.372–2.507	2.338–2.540	1.4
$\sin^2\theta_{23}/10^{-1}$	NO	5.51	4.81–5.70	4.48–5.88	4.30–6.02	5.2
	IO	5.57	5.33–5.74	4.86–5.89	4.44–6.03	4.8
δ/π	NO	1.32	1.14–1.55	0.98–1.79	0.83–1.99	14.6
	IO	1.52	1.37–1.66	1.22–1.79	1.07–1.92	9.3

CP violation. CP conservation is generally disfavored, but remains allowed at $\sim 2\sigma$ in NO. The octant of θ_{23} is unresolved at the $\sim 2\sigma$ level in both NO and IO. If these trends are confirmed, the mass spectrum ordering and the CP phase δ might be the first "unknowns" to become "known" (at $> 3\sigma$) with further data; assessing the octant and excluding CP conservation might instead require more effort.

We conclude this section by comparing our results with other recent global analyses [31–33]. If we exclude SK atmospheric data as advocated in [31,32], our results agree well with theirs on both known and unknown parameters. In particular, we obtain very similar χ^2 curves for δ and for θ_{23}, including a comparable offset $\Delta\chi^2$ between IO and NO (not shown). Given this agreement, we surmise that the authors of [31,32] would also obtain results very similar to ours (Fig. 3 and Table 1) by adding the χ^2 map from the latest SK atmospheric neutrino data [177] in their recent fit [32]. Concerning the analysis in [33], we observe qualitative agreement with their hints on the mass ordering and the CP-violating phase. However, at the level of details, a comparison with [33] is not obvious: their dataset is based on earlier T2K and NOvA data, and it also includes the χ^2 map of older SK atmospheric data [176], that was derived in the approximation $\delta m^2 = 0$. By construction, this approximation switches off CP-violation effects (and may bias other subleading effects) in atmospheric neutrinos, preventing a proper and detailed comparison of global fit results.

4. Results on oscillation parameter pairs

In this Section we show the allowed regions in various planes charted by pairs of oscillation parameters. We discuss covariances related to δm^2-driven oscillations, to Δm^2-driven oscillations, and to the CP-violating phase δ. We always take NO and IO as two isolated cases, without marginalizing over the mass ordering.

4.1. Covariances of $(\delta m^2,\ \theta_{12}, \theta_{13})$

The $(\delta m^2,\ \theta_{12}, \theta_{13})$ parameters govern the oscillations of solar and KamLAND neutrinos, which are of great importance not only by themselves but also for providing the $(\delta m^2,\ \theta_{12})$ input to the full 3ν analysis of all the other experiments.

Fig. 4 shows the $N\sigma$ regions allowed separately by solar and KamLAND data in the plane $(\delta m^2,\ \sin^2\theta_{12})$, assuming NO and fixing θ_{13} at a representative value ($\sin^2\theta_{13} = 0.02$). The separate results show some slight tension between the preferred mass-mixing values (between 1σ and 2σ from a glance at Fig. 4), that has received interest (see, e.g., [108,197–199]) as a possible indication of nonstandard neutrino interactions in the solar matter (see, e.g., [200–204]). We remind that nonstandard four-fermion interactions with effective couplings $\varepsilon_{\alpha\beta}G_F$ (typically with $|\varepsilon_{\alpha\beta}| \ll 1$), may affect the precise determination of the oscillation parameters: in particular, flavor-diagonal couplings ($\alpha = \beta$) tend to affect the neutrino energy differences and thus the squared mass gaps, while off-diagonal couplings ($\alpha \neq \beta$) tend to alter the mixing matrix in matter [37,205]. In the vast related literature, see, e.g., [206–210] for phenomenological reviews and [211–213] for theoretical model constructions.

We quantify the tension between the best fits in Fig. 4 in terms of the difference between the joint and separate χ^2 minima, $\Delta\chi^2 = \chi^2_{\text{solar+KL}} - (\chi^2_{\text{solar}} + \chi^2_{\text{KL}}) \simeq 2$, finding $N\sigma \simeq 1.4$; this value would slightly increase to $N\sigma = 1.6$ for unconstrained θ_{13} (using only solar and KL data). We conclude that the overall hint in favor of nonstandard interactions in the Sun does not exceed 2σ at present. Should this hint be corroborated by future data, nonstandard interactions should be generally considered also in the Earth matter, and they could affect future measurements of the known $(\Delta m^2,\ \theta_{23},\ \theta_{13})$ parameters, or perturb indications about the unknown mass ordering. This possibility provides a relevant example of the interplay between the 3ν oscillation parameters and generalized "unknowns" coming from scenarios beyond 3ν, which provide an active area of research for prospective oscillation searches; see, e.g., [210,214–220] for recent studies.

Let us now discuss the details of the 3ν mass-ordering effects in Fig. 4. This figure has been obtained for NO; in IO the KamLAND contours would not change, since Δm^2-driven oscillations are effectively averaged out, and the sign of Δm^2 is not

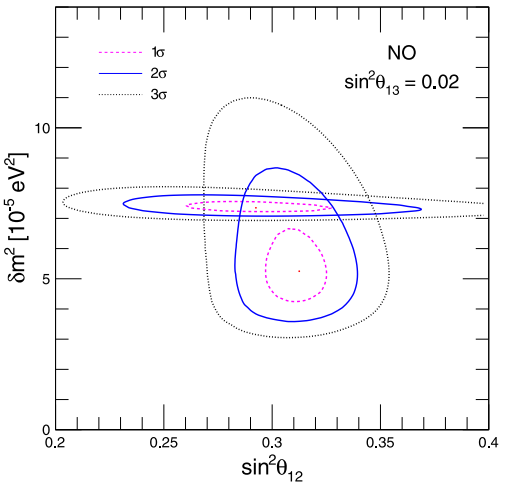

Fig. 4. Separate analysis of solar and KamLAND neutrino experiments in the plane $(\delta m^2,\ \sin^2\theta_{12})$, assuming NO and a fixed value $\sin^2\theta_{13} = 0.02$. The contours correspond to $N\sigma = 1,\ 2,\ 3$. For IO, the solar neutrino contours would be very similar, but shifted by $\delta(\sin^2\theta_{12}) \simeq -0.02$ (not shown). See the text for details.

probed [see Eq. (12)]. However, for solar neutrinos, Eq. (12) involves the effective θ_{13} mixing angle in matter, which embeds a slight residual dependence on $\pm\Delta m^2$ [114] and thus to mass ordering [1]. We find that the solar neutrino contours in Fig. 4 would be slightly different in IO, being basically shifted leftwards by a tiny amount, $\delta(\sin^2\theta_{12}) \simeq -0.02$ (not shown). This small shift compensates, in the solar neutrino data fit, the slightly higher survival probability for IO as compared to NO (see Fig. 13 in [114]). In combination with (mass-ordering insensitive) KamLAND data, the overall shift of the best-fit mixing angle amounts to $\delta(\sin^2\theta_{12}) \simeq -0.01$ in IO, as also reported in Table 1 for the sake of precision. The absolute χ^2 difference between the solar+KL fit amounts to a mere $\Delta\chi^2 = 0.08$ in favor of IO with respect to NO; although statistically insignificant, this difference has been taken into account in our global analysis.

We conclude our comments to Fig. 4 by noting that analogous results shown in [84] (see Figs. 33 and 34 therein) display solar neutrino contours with small "wiggles" that are not found in other recent analyses [31–34]. We surmise that such wiggles are not physical effects (which should be smoothly varying in terms of δm^2), but may be numerical artifacts due to insufficient grid sampling in an integration variable (either energy or zenith angle). In this specific case, an "official" χ^2 map from the collaboration would not bring a clear advantage over analyses performed by external researchers, in terms of overall accuracy.

We now consider the covariances of any pair of parameters among $(\delta m^2,\ \theta_{12},\ \theta_{13})$, as obtained by considering increasingly rich datasets. Fig. 5 shows the covariances as obtained by solar+KL data only, which provide the well-known weak hint $(\sim 1\sigma)$ for nonzero θ_{13} [16], with negligible correlations of θ_{13} with the other two parameters.

Fig. 6 is analogous to Fig. 5 but includes long-baseline accelerator data, that provide a dramatic reduction of the allowed range for θ_{13} due to flavor-appearance data. The small kink in the contours involving the θ_{13} parameter has a physical origin, being related to the octant degeneracy of θ_{23}: in a sense, the contours in the planes involving θ_{13} are superpositions of two regions, slightly displaced in θ_{13}, corresponding to nearly-degenerate fits in the two θ_{23} octants. See also Fig. 1, as well as the discussion of the correlations between θ_{23} and θ_{13} in the next subsection.

Fig. 7 is analogous to Fig. 6 but includes short-baseline reactor data, that provide further dramatic reduction of the allowed range for θ_{13} as compared with Figs. 5 and 6. In this context, the inclusion of atmospheric neutrino data (not shown) would not induce any appreciable variation with respect to Fig. 7. A further reduction of the θ_{13} allowed range is expected from the final (and possibly combined) datasets collected by the running reactor experiments [143,144], while a very significant reduction of the $(\delta m^2,\ \theta_{12})$ range will be possible in the medium-baseline JUNO experiment (in construction) [192].

4.2. *Covariances of* $(\Delta m^2,\ \theta_{23}, \theta_{13})$

The covariances of parameter pairs among $(\Delta m^2,\ \theta_{23}, \theta_{13})$ help to understand the interplay of different datasets in producing various single-parameter results discussed in Section 3. Since there are appreciable differences in NO and IO, we show both cases in the following figures.

Fig. 8 shows the regions allowed at $N\sigma$ in the plane charted by $(\sin^2\theta_{23},\ \sin^2\theta_{13})$, for both NO (upper panels) and IO (lower panels), for increasingly rich datasets (panels from left to right). The leading LBL appearance amplitude in Eq. (13), governed by the $\sin^2\theta_{23}\sin^2\theta_{13}$, induces an anti-correlation between these two parameters, visible in the left panels. Subleading effects sensitive to sign(Δm^2) [second and third row of Eq. (13)] generate a difference in the allowed θ_{13} ranges for NO and IO, the latter ones being generally higher. The middle panels show the combination with SBL reactor data. The comparison of the

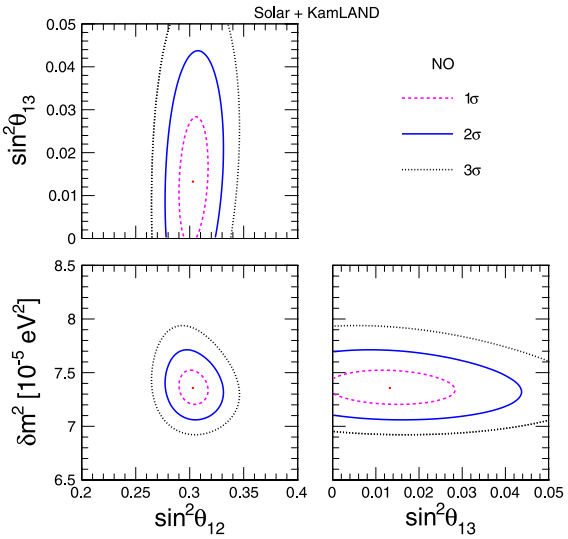

Fig. 5. Joint analysis of solar and KamLAND neutrino data in each of the planes charted by one pair of parameters among $(\delta m^2,\ \sin^2\theta_{12},\ \theta_{13})$. The contours correspond to $N\sigma = 1,\ 2,\ 3$. Results refer to NO, and would be very similar for IO (not shown). See the text for details.

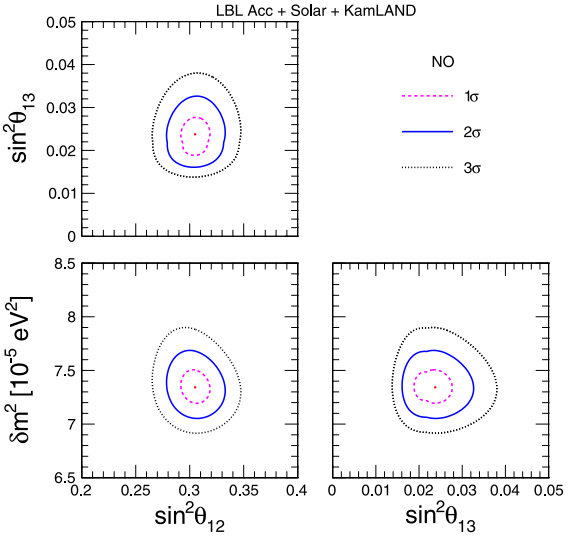

Fig. 6. As in Fig. 5, but adding long-baseline accelerator data in the analysis.

left and middle panels shows that current accelerator and reactor constraints on θ_{13} are more consistent in NO than in IO. This fact provides the increment of the $\Delta\chi^2$ difference from Eq. (16) to Eq. (17). Atmospheric neutrino data cannot improve θ_{13} further, but remain sensitive to the mass ordering and provide an independent $\Delta\chi^2$ increment from Eq. (17) to Eq. (18). Concerning θ_{23}, note that the slight θ_{13} tension between accelerator and reactor data in IO; such tension is minimized for relatively large θ_{23}, hence the more pronounced preference for the second octant. In any case, the octant ambiguity remains unresolved at 2σ level in both NO and IO.

Fig. 9 shows the covariance of the $(\Delta m^2,\ \sin^2\theta_{23})$ parameters, in the same format as Fig. 8. A striking feature of the NO case (upper panels) is the very good consistency of all the data on Δm^2, whose best-fit value remains practically constant in the three upper panels. In IO (lower panels) the value of Δm^2 slightly increases after the addition of SBL reactor data, as consequence of the slight increment in $\sin^2\theta_{23}$ discussed for Fig. 8. This small increase of Δm^2 slightly worsen the agreement with IC-DC data, that tend to prefer relatively low values of Δm^2 [172]. Thus the IC-DC dataset also provides a small contribution to the $\Delta\chi^2$ (about one unit) favoring NO in Eq. (18). Note that, in general, at nearly maximal mixing one gets the lowest allowed values of Δm^2, while for nonmaximal mixing (in either octants) the preferred values of Δm^2 tend to increase. This correlation stems mainly from disappearance data in LBL accelerator experiments, where a decrease of the

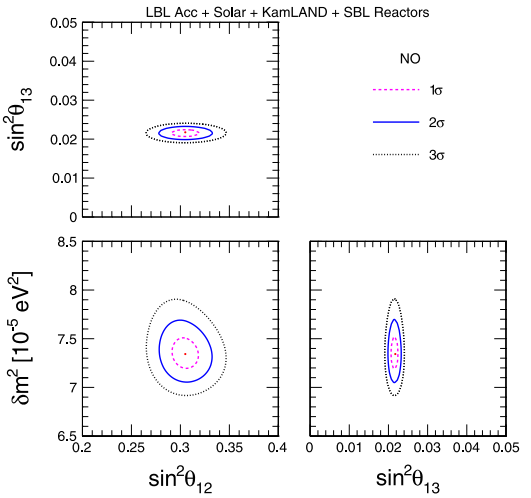

Fig. 7. As in Fig. 6, but adding short-baseline reactor data in the analysis.

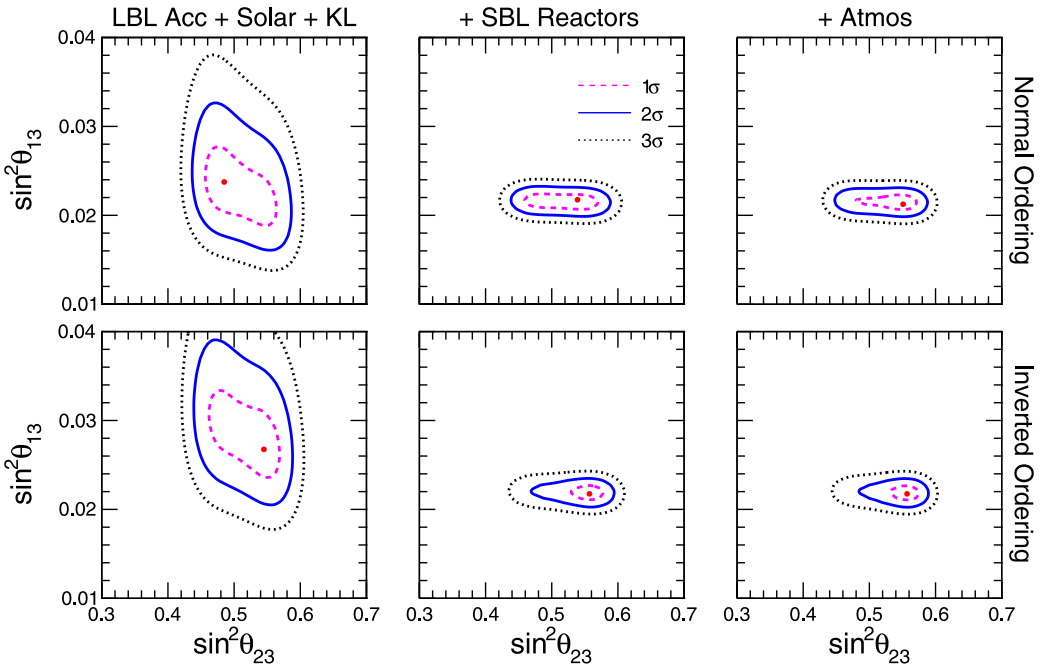

Fig. 8. Covariance plot for the ($\sin^2\theta_{13}$, $\sin^2\theta_{23}$) parameters in NO (upper panels) and IO (lower panels), as derived from an analysis of LBL accelerator + solar + KL data (left panels), plus SBL reactor data (middle panels), plus atmospheric neutrino data (right panels).

leading oscillation amplitude (governed by $\sin^2 2\theta_{23}$) can be partly traded for an increase of the leading oscillations phase (governed by Δm^2), so as to keep the disappearance rate nearly constant.

Fig. 10 shows the covariance of the (Δm^2, $\sin^2\theta_{13}$) parameters. In the left panels, one can notice the mentioned preference for higher values of θ_{13} in IO, as well as a small kink in the contours. This feature shares the same origin as the kink discussed in the context of Fig. 6, namely, the contours correspond to two slightly displaced allowed ranges for θ_{13}, related to nearly-degenerate fits in the θ_{23} octants. Such kink disappears with the addition of SBL reactor data.

Summarizing, Figs. 8–10 show the interplay among the (Δm^2, θ_{23}, θ_{13}) parameters within different datasets. In the NO case there is very good agreement among the values of both Δm^2 and θ_{13} from different datasets, and θ_{23} remains nearly maximal at 1σ, with a minor preference for the second octant. In IO there is a slight tension between accelerator and reactor constraints on θ_{13}, which contributes to disfavor IO and to slightly prefer the second octant of θ_{23}—these two trends being corroborated by atmospheric data. However, even in IO, the octant degeneracy remains unresolved at 2σ.

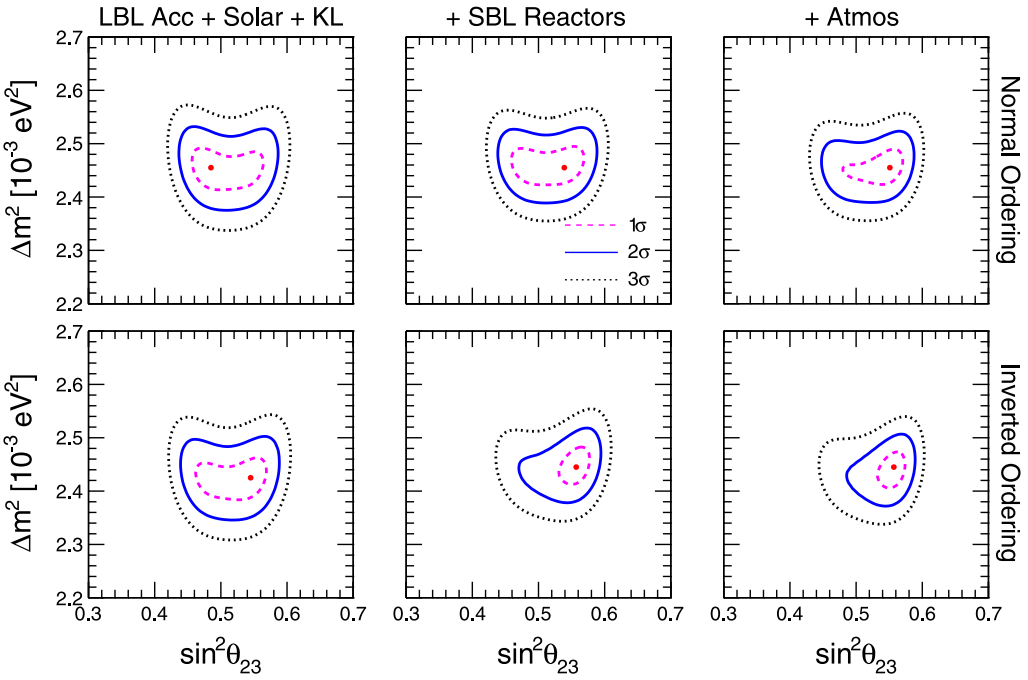

Fig. 9. Covariance of the $(\Delta m^2,\ \sin^2\theta_{23})$ parameters.

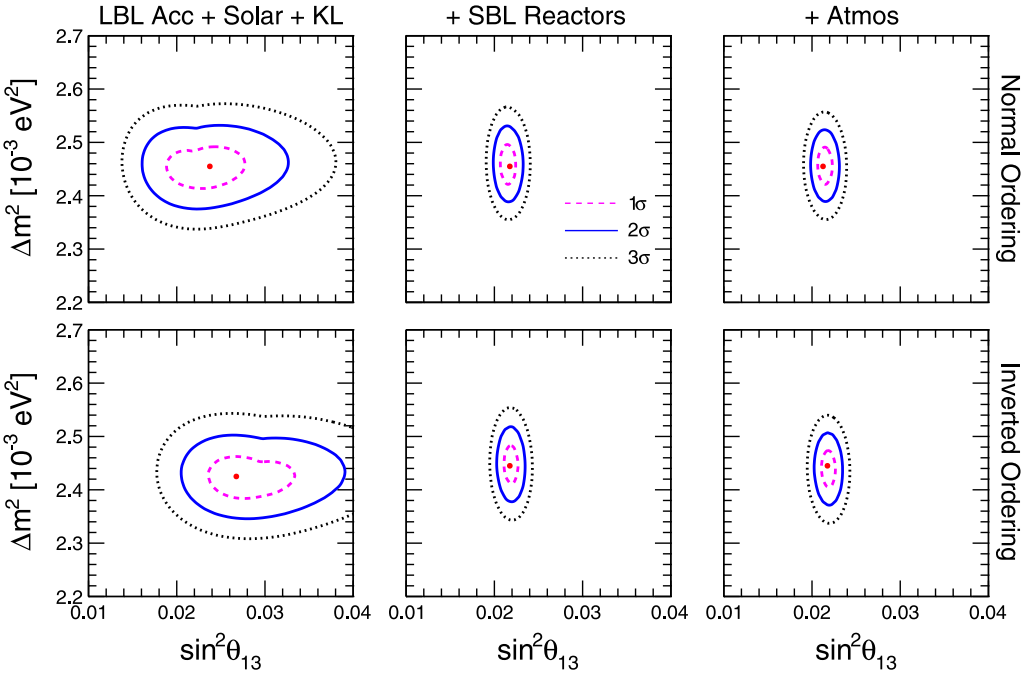

Fig. 10. Covariance of the $(\Delta m^2,\ \sin^2\theta_{13})$ parameters.

A final remark is in order. The previous description of fine details (at the 1σ–2σ level) in the covariances of the known parameters $(\Delta m^2,\ \theta_{23}, \theta_{13})$ is based on the assumption of standard 3ν oscillations. At the same level of detail, possible new neutrino physics (such as nonstandard interactions discussed before) might induce noticeable changes and could shift the best fits, alter the various hints, or spoil the apparent data agreement. The fragility of fit details (at 1σ–2σ level) under such possible perturbations should always be kept in mind.

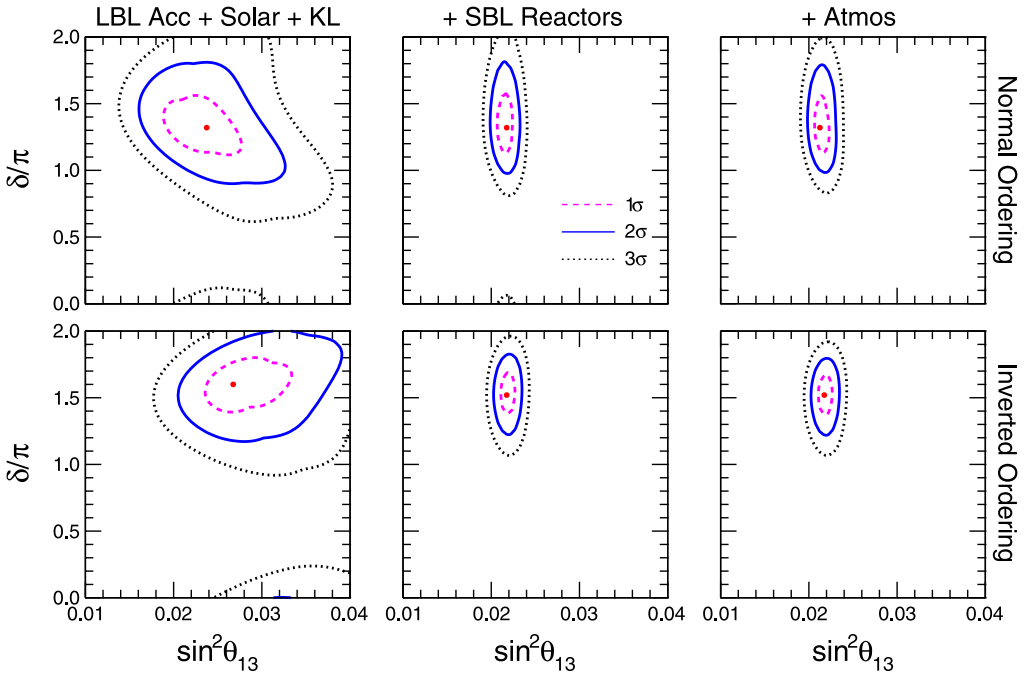

Fig. 11. Covariance of the $(\delta,\ \sin^2\theta_{13})$ parameters.

4.3. Covariances involving δ

We complete our analysis of covariances by discussing those involving the unknown parameter δ and one of the two known mixing angles $(\theta_{13},\ \theta_{23})$. There is a vast literature on analytical studies of such correlations, the works in [221–223] providing just a few recent examples among many. Here we focus on the phenomenological correlations stemming from current data.

Fig. 11 shows the $N\sigma$ regions allowed in the plane $(\delta,\ \sin^2\theta_{13})$. The strong correlations between these two parameters (in the left panels) are mainly induced by the interplay between δ and θ_{13} arising in the subleading terms (second and third row) of Eq. (13). In NO, the best fit of δ remains very close to $\sim\ 1.3\pi$ by adding first SBL reactor and then atmospheric neutrino data. In NO, the consistency of all the datasets towards the same best-fit values of both the known $(\Delta m^2,\ \theta_{23}, \theta_{13})$ parameters and of the unknown δ phase is striking. In IO there is a slight decrease of δ from left to middle panels, correlated to the decrease of θ_{13}.

Fig. 12 shows the $(\delta,\ \sin^2\theta_{23})$ covariance. Only weak correlations (if any) emerge between these two parameters at the current level of accuracy; see, e.g., [223] for prospective improvements. In particular, in NO there is a slight anti-correlation, which implies that the best fit of δ might increase from $\sim\ 1.3$ to $\sim\ 1.4$ if the first (rather than the second) octant of θ_{23} were favored by upcoming data. In IO there is no significant correlation. These considerations about the interplay among three unknowns (the phase δ, the θ_{23} octant and the mass ordering) are rather fragile and might change with future data. Conversely, the overall 3σ constraints on δ emerging in Figs. 11 and 12 appear to be relatively robust, with modest dependence on $(\theta_{13},\ \theta_{23})$.

In a sense, the CP phase is already being "measured" by current experiments, with an effective 1σ accuracy of $\sim$ 15% in NO and $\sim$ 9% in IO (see also Table 1). In the favored case of NO, this accuracy is sufficient to reject the CP-conserving case $\delta = 0\,(\text{or}\ 2\pi)$ at 3σ, but is not enough to exclude the other CP-conserving case $\delta = \pi$ at 2σ. Both cases are instead excluded at 3σ in the IO case that, however, is in turn disfavored with respect to NO case, see Eq. (18). Summarizing, although CP conservation cannot be rejected yet with significant confidence, relatively stringent constraints on δ can be obtained from current data, with a clear preference for $\sin\delta < 0$.

The progress made by CP-sensitive oscillation searches is impressive: in contrast, a dozen years ago the CP-conserving cases were found to be largely degenerate at $< 1\sigma$ level, with no significant difference between NO and IO [1]. If this exciting trend continues, there are good prospects to eventually assess CP violation at $> 3\sigma$ with future data.

We conclude this section with some comments on scenarios beyond 3ν. As we have seen, there is a high degree of convergence of all the data within the standard 3ν framework, which implies that new physics effects, if any, must remain small as compared with the estimated uncertainties. In particular, apart from the mild tension between solar and KL results discussed earlier, there are no relevant anomalous results pointing towards new neutrino interactions, whose couplings and other features can be thus constrained by oscillation (plus other) data.

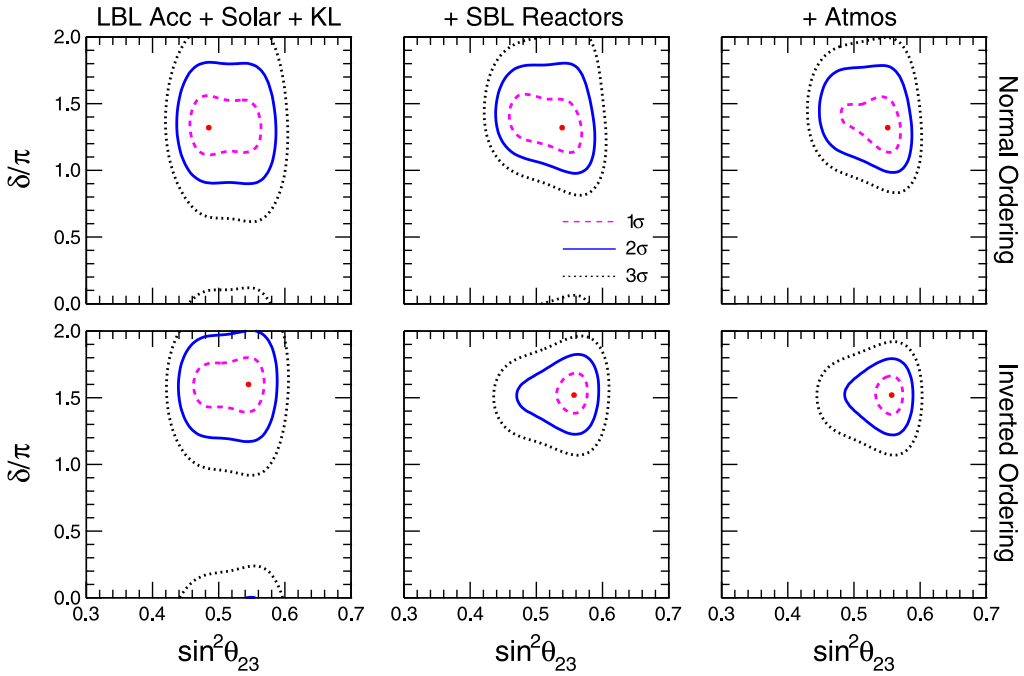

Fig. 12. Covariance of the $(\delta,\ \sin^2\theta_{23})$ parameters.

The situation is somewhat different concerning new neutrino states, since there are long-standing anomalies that seem to point towards a 4th massive (so-called sterile) state at the $O(1)$ eV scale, slightly mixed with both ν_e and ν_μ; see [59,224] for reviews. This exciting possibility is balanced by internal tensions between different datasets (especially appearance versus disappearance) within the 4ν oscillation scenario and its variants; see [60,61] for recent goodness-of-fit assessment and parameter estimates. A large experimental investment is being made to clarify this puzzling situation, and interesting new results are expected by a variety of short-baseline oscillation searches [225,226]. In this context, it is worth reminding that the 3×3 matrix in Eq. (1) would become non-unitary in the presence of new states at the eV scale or higher, with new mixing angles and CP phases inducing effects degenerate with the standard 3ν ones, see e.g. [227–234]. In particular, the determination of δ, the discrimination of the mass hierarchy and the resolution of the octant of θ_{23}, appear to be quite sensitive to such additional unknowns, see [235–241] for recent studies. Settling the status of sterile neutrino oscillations will thus be beneficial to gain more confidence in current hints about 3ν unknowns.

5. Constraints from non-oscillation data and combination with oscillation searches

Nonoscillation data from single β decay, $0\nu\beta\beta$ decay and cosmology are crucial to probe the nature and absolute masses of neutrinos, which are not accessible via flavor oscillations. They also offer additional handles to probe the neutrino mass ordering and to check the consistency of 3ν framework [242,243]. Within the 3ν scenario, the available beta-decay bounds are the level $m_\beta < 2$ eV [3], while typical mass bounds placed by $0\nu\beta\beta$ decay and cosmology are the sub-eV level [56,244,245]. Therefore we shall consider only the experimental bounds on Σ and on $m_{\beta\beta}$ (the latter being valid if neutrinos are Majorana).

We follow the same 3ν (frequentist) methodology as in [35], based on the construction of χ^2 functions for m_β and Σ, to be added to the χ^2 function coming from the previous oscillation data analysis, marginalized over all the known and unknown mass-mixing parameters and phases. There are alternative approaches to absolute mass observables based on Bayesian statistics (see, e.g., [246–249]), whose results depend somewhat on prior assumptions. As already remarked for oscillation observables we underline that, irrespective of statistical details, possible new neutrino states and interactions (not considered herein) might profoundly affect our understanding of non-oscillation observables [250].

5.1. Inputs from neutrinoless double beta decay and cosmology

Running $0\nu\beta\beta$ experiments have not found evidence for this rare process so far [54,251–255], and the quest for the neutrino nature (Dirac or Majorana) remains open. If neutrinos are Majorana, within the 3ν framework one can translate lower limits on the decay half life into upper limits on $m_{\beta\beta}$, via the knowledge of the nuclear matrix element (NME) for the considered nucleus [54–56] Improving the NME calculations and the underlying nuclear models is imperative to get

significant constraints on $m_{\beta\beta}$ [256]. In this context, the poorly known value of the effective axial coupling g_A in the nuclear medium is being increasingly recognized as one of the most serious issues in the field [54,256,257], to be addressed with a variety of theoretical and experimental tools also involving other weak-interaction nuclear processes [258].

Despite the relatively large uncertainties on the NME's, it is fair to say that the leading upper limit on $m_{\beta\beta}$ is currently placed by the KamLAND-Zen experiment using ^{136}Xe [251]. We convert its data into a function $\chi^2(m_{\beta\beta})$ according to the procedure in [35], which marginalizes away the conservative NME errors (including g_A uncertainties) estimated in [259]. As a representative result we quote the 2σ upper limit (which applies to both NO and IO) [35],

$$m_{\beta\beta} < 0.18 \text{ eV at } 2\sigma \ . \tag{19}$$

Concerning cosmology, we adopt the same experimental inputs and analysis results reported in the recent paper [35]. The analysis was based on six combinations of data coming from the so-called TT, TE and EE anisotropy angular power spectra of Planck [260], where T and E refer to temperature and polarization, respectively. Such Planck data were eventually supplemented with lensing potential power spectrum reconstruction data, and with optical depth HFI constraints ($\tau_{\rm HFI}$) [261]. Also considered were baryon acoustic oscillation (BAO) measurements [262–264]. The adopted cosmological framework was based on the so-called ΛCDM model, with allowance for massive neutrinos (ΛCDM+Σ). Systematic uncertainties affecting the ΛCDM+Σ model were lumped in a dominant parameter $A_{\rm lens}$ (with significant covariance with Σ), that was optionally left free to vary around its standard value ($A_{\rm lens} = 1$), in order to improve the overall fit of Planck lensing data [265].

In the work [35], a total of 6+6 datasets (with and without free $A_{\rm lens}$) were thus considered. In combination with oscillation data, upper limits at 2σ were obtained for these 12 cases, mostly in the sub-eV range for the ΛCDM+Σ model, with somewhat weaker results for ΛCDM+Σ+$A_{\rm lens}$ variants. Allowance was given for different (non-degenerate) neutrinos masses, inducing small differences between the overall χ^2 in NO and IO at small Σ. Interestingly, NO was generally favored over IO, although only by a fraction of $\Delta\chi^2$ unit in typical cases. These results (in particular, the numerical values in Table II of [35]) are confirmed by including the updated oscillation data discussed above, and are not repeated.

Among the twelve cases reported in [35], we discuss here only the two cases labeled 1 and 6 in the ΛCDM+Σ model. They provide representative example of "weak" cosmological upper limits (just below the eV scale), and "strong" cosmological upper limits (in the sub-eV range). The corresponding χ^2 functions are taken from [35] for both NO and IO, and provide the following 2σ upper limits:

$$\text{"weak" limit} : \ \Sigma < 0.72 \text{ (NO) or } \Sigma < 0.80 \text{ (IO) at } 2\sigma \ , \tag{20}$$

$$\text{"strong" limit} : \ \Sigma < 0.18 \text{ (NO) or } \Sigma < 0.20 \text{ (IO) at } 2\sigma \ . \tag{21}$$

As already emphasized, we discuss NO and IO separately, and do not consider anymore the marginalized "any ordering" case [35], which would display only NO regions (and no IO region) up to 3σ.

5.2. Representative bounds on $(m_\beta,\ m_{\beta\beta},\ \Sigma)$

Fig. 13 shows the results of a combined 3ν analysis of oscillation and nonoscillation data, in the planes charted by any pair among the absolute mass observables $(m_\beta,\ m_{\beta\beta},\ \Sigma)$, for the "weak" cosmological limit described above. The allowed bands correspond to 2σ (solid) and 3σ (dotted), for both NO (blue) and IO (red). Note the spread in $m_{\beta\beta}$ at any fixed value of m_β or of Σ, induced by the unknown Majorana phases. In the plane $(\Sigma,\ m_{\beta\beta})$, there is an interesting synergy between the upper bounds on these two parameters, coming from cosmological and $0\nu\beta\beta$ data, respectively: the first would cut the allowed band vertically, while the second horizontally, their combination providing a "slanted" upper limit to the allowed band. The other two panels show also the projection onto the m_β variable, with 2σ upper limits slightly above 0.2 eV. This fraction of the m_β allowed range can be probed by the KATRIN experiment (in construction) [266].

Fig. 14 is analogous to Fig. 13, but refers to the "strong" cosmological limit described above. This limit dominates over the $0\nu\beta\beta$ bound in the fit and, in the $(\Sigma,\ m_{\beta\beta})$ plane, it provides a vertical cut to the allowed bands. In the $(\Sigma,\ m_\beta)$ plane, the narrow bands for NO and IO are completely separated. At least in principle, precise $(\Sigma,\ m_\beta)$ measurements could then be able to select one mass ordering. Unfortunately, the allowed m_β range is well below the KATRIN sensitivity, although it might be partly accessed with future projects based on new detector concepts [267–269]. Note that cosmology could select NO at 2σ, if the upper bound were reduced by a factor of two.

Summarizing, measurements of $(m_\beta,\ m_{\beta\beta},\ \Sigma)$ have the potential to test the 3ν paradigm and its three mass-related unknowns: the fundamental nature of the mass term, the absolute neutrino mass scale, and the mass ordering. The first unknown remains as such, both options (Dirac or Majorana) being possible in the absence of a $0\nu\beta\beta$ decay signal. The second unknown remains also undetermined, but with upper limits which are steadily decreasing and will eventually hit the signal. The third unknown is being approached by cosmology, although only weakly at present—the preference for NO being mainly driven by current oscillation data.

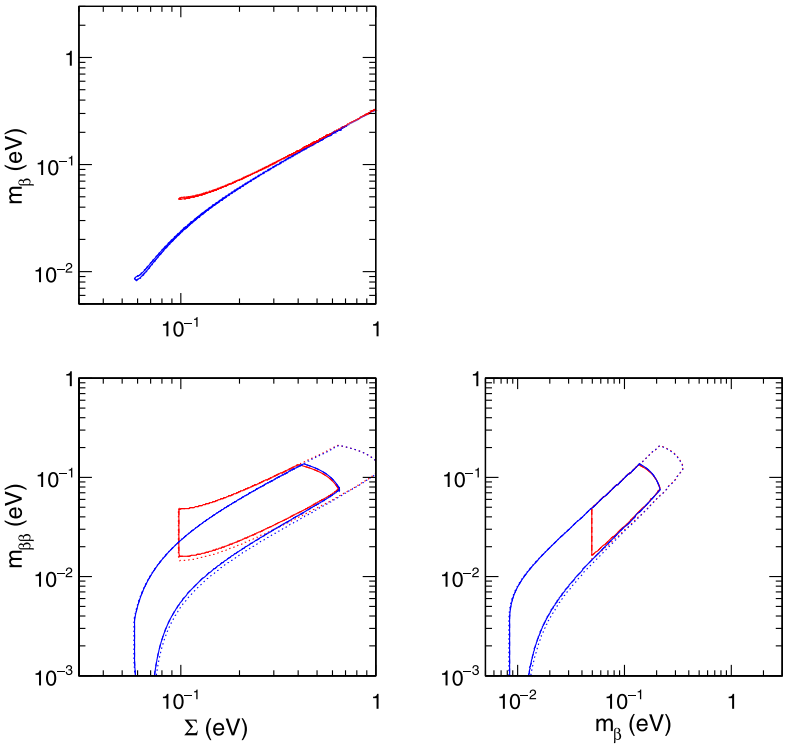

Fig. 13. Combined 3ν analysis of oscillation and nonoscillation data, in the planes charted by any pair among the absolute mass observables (m_β, $m_{\beta\beta}$, Σ). Bounds from $0\nu\beta\beta$ are derived from KamLAND-Zen data and NME estimates. Bounds from cosmology refer to the representative "weak" limit described in the text. The allowed bands correspond to $N\sigma = 2$ (solid) and $N\sigma = 3$ (dotted), for both NO (blue) and IO (red), taken as separate cases. If the $\Delta\chi^2_{\text{IO–NO}}$ difference in Eq. (18) was included, the IO bands would disappear. (For interpretation of the references to color in this figure legend, the reader is referred to the web version of this article.)

6. Summary and conclusions

We have presented an up-to-date global analysis of data coming from neutrino oscillation and non-oscillation experiments, as available in April 2018, within the standard framework including three massive and mixed neutrinos. We have discussed in detail the status of the three-neutrino (3ν) mass-mixing parameters, both known and unknown, as listed in Eqs. (9) and (10).

The main results from the analysis of oscillation searches are summarized graphically in Fig. 3 and numerically in Eq. (18) and Table 1. Concerning the known parameters: the squared mass differences (δm^2, $|\Delta m^2|$) are determined within a couple of percent, while the mixing parameters ($\sin^2\theta_{12}$, $\sin^2\theta_{13}$, $\sin^2\theta_{23}$) within a few percent; see the last column in Table 1 for more precise values. Concerning the unknown parameters: a preference for NO emerges at 3σ level from the global analysis, with coherent contributions from various datasets. If the $\Delta\chi^2$ difference in Eq. (18) is taken at face value, no allowed region survives for IO up to 3σ. By considering NO and IO as separate cases, we also find that the Dirac CP phase δ is constrained within $\sim 15\%$ ($\sim 9\%$) uncertainty in NO (IO) around nearly-maximal CP-violating values, $\delta \sim 3\pi/2$. The CP-conserving value $\delta = 0$ (or 2π) is disfavored at 3σ in both NO and IO; the value $\delta = \pi$ is also disfavored at 3σ in IO but not in NO (where it is still allowed at 2σ). Concerning deviations of θ_{23} from maximal mixing, we find an overall preference for the second octant (more pronounced in IO), although both octants are allowed at 2σ.

The above results have been discussed in detail in terms of increasingly rich datasets and of covariance plots between various pairs of parameters. We have also tried to convey the message that oscillation data analyses are becoming increasingly complicated to be performed outside the experimental collaborations. External users may need to adopt officially processed results, e.g., in terms of χ^2 maps when available. In this work, we have used such maps for Day Bay reactor results, as well as for Super-Kamiokande and IceCube-DeepCore atmospheric results. However, the integration of raw data and processed results should always be performed in a critical way. We have argued that progress in the field of data analyses requires an advanced discussion of theoretical and experimental uncertainties, at the same level of refinement of other mature fields in particle physics. Such progress is crucial to probe further the emerging hints on the unknown 3ν oscillations parameters. We have also remarked that these hints may be perturbed by possible new states and interactions beyond the standard 3ν framework.

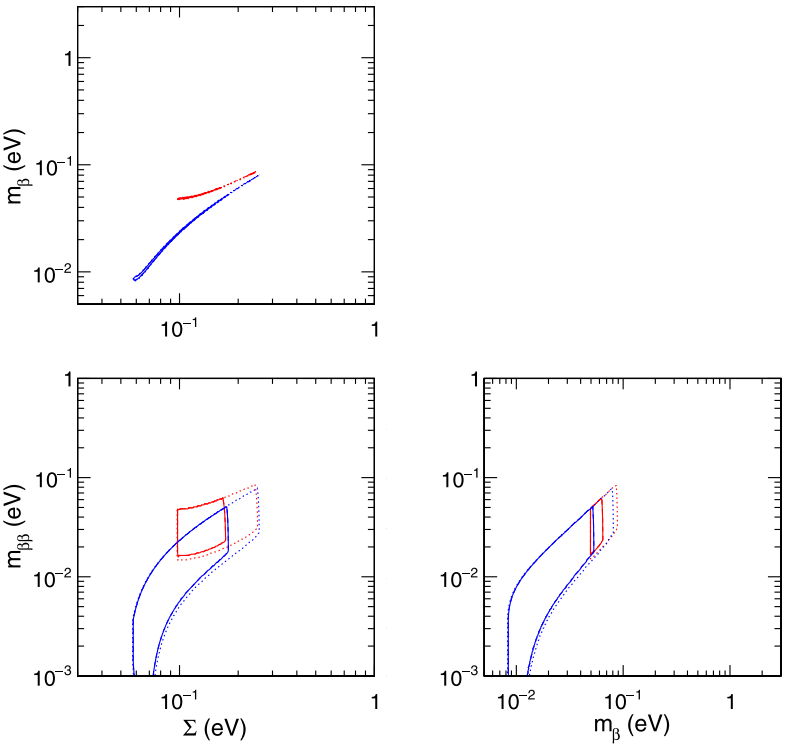

Fig. 14. As in Fig. 13, but for "strong" cosmological limits as described in the text.

Concerning the non-oscillation observables (m_β, $m_{\beta\beta}$, Σ), the combination with oscillation constraints has been shown for two representative cases, corresponding to "weak" and "strong" bounds from cosmology, in Figs. 13 and 14 respectively. In the absence of a $0\nu\beta\beta$ signal, the Dirac or Majorana nature of massive neutrinos remains undetermined. The absolute neutrino mass scale is also undetermined, but with upper limits that are steadily decreasing. For "weak" cosmological bounds, a fraction of the allowed regions can be probed by direct mass searches. Limits from cosmology appear rather promising, as a reduction of the "strong" bounds by a factor of two might approach the threshold for NO–IO separation.

In conclusion, the 3ν mass-mixing paradigm is being probed with increasing accuracy. The known oscillation parameters are determined with a few percent precision, and statistically significant hints are emerging on the mass ordering and on the CP-violating Dirac phase. The progress made in a dozen years since a previous review in this Journal [1] is impressive. We look forward to seeing the completion of the 3ν framework, as well as hints (and possible signals) coming from absolute mass observables in the future. Possible indications of new physics beyond the 3ν paradigm might also emerge, and provide surprising and novel directions for global analyses.

Acknowledgments

We thank E. Di Valentino and A. Melchiorri for permission to use the cosmological likelihood functions previously derived and presented in [35]. We are grateful to various members of experimental collaborations for informing us about the public release of their official neutrino oscillation data analyses, including: M. Nakahata, T. Nakaya and D. Wark (Super-Kamiokande atmospheric data), E. Resconi and T. DeYoung (IceCube DeepCore atmospheric data), and D. Naumov (Daya Bay reactor data).

A.P. is supported by the grant "Future In Research" *Beyond three neutrino families*, Fondo di Sviluppo e Coesione 2007–2013, APQ Ricerca Regione Puglia, Italy, "Programma regionale a sostegno della specializzazione intelligente e della sostenibilità sociale ed ambientale". E.L., A.M. and A.P. acknowledge partial support by the research project TAsP (Theoretical Astroparticle Physics) funded by the Istituto Nazionale di Fisica Nucleare (INFN). F.C. acknowledges partial support by the Deutsche Forschungsgemeinschaft through Grant No. EXC 153 (Excellence Cluster "Universe") and Grant No. SFB 1258 (Collaborative Research Center "Neutrinos, Dark Matter, Messengers") as well as by the European Union through Grant No. H2020-MSCA-ITN-2015/674896 (Innovative Training Network "Elusives").

References

[1] G.L. Fogli, E. Lisi, A. Marrone, A. Palazzo, Prog. Part. Nucl. Phys. 57 (2006) 742. hep-ph/0506083.
[2] C. Patrignani, et al. [Particle Data Group], Chin. Phys. C 40 (10) (2016) 100001.
[3] K. Nakamura, S. Petcov, Neutrino Masses, Mixing, and Oscillations, in [2].
[4] 2015 Nobel prize https://www.nobelprize.org/nobel_prizes/physics/laureates/2015/.
[5] T. Kajita, Rev. Modern Phys. 88 (3) (2016) 030501.
[6] A.B. McDonald, Rev. Modern Phys. 88 (3) (2016) 030502.
[7] 2016 Breakthrough prize, website https://breakthroughprize.org/Laureates/1/P1/Y2016.
[8] L.J.W.J. Cao, Y.F. Wang, Ann. Rev. Nucl. Part. Sci. 67 (2017) 183 arXiv:1803.10162 [hep-ex].
[9] M.V. Diwan, V. Galymov, X. Qian, A. Rubbia, Ann. Rev. Nucl. Part. Sci. 66 (2016) 47 arXiv:1608.06237 [hep-ex].
[10] B. Pontecorvo, Sov. Phys.—JETP 26 (1968) 984; Zh. Eksp. Teor. Fiz. 53 (1967) 1717.
[11] Z. Maki, M. Nakagawa, S. Sakata, Progr. Theoret. Phys. 28 (1962) 870.
[12] C. Giganti, S. Lavignac, M. Zito, Prog. Part. Nucl. Phys. 98 (2018) 1 arXiv:1710.00715 [hep-ex].
[13] C. Jarlskog, Phys. Rev. Lett. 55 (1985) 1039.
[14] N. Cabibbo, Phys. Lett. 72B (1978) 333.
[15] M. Apollonio, et al. [CHOOZ Collaboration], Eur. Phys. J. C 27 (2003) 331. hep-ex/0301017.
[16] G.L. Fogli, E. Lisi, A. Marrone, A. Palazzo, A.M. Rotunno, Phys. Rev. Lett. 101 (2008) 141801 arXiv:0806.2649 [hep-ph].
[17] K. Abe, et al. [T2K Collaboration], Phys. Rev. Lett. 107 (2011) 041801 arXiv:1106.2822 [hep-ex].
[18] P. Adamson, et al. [MINOS Collaboration], Phys. Rev. Lett. 107 (2011) 181802 arXiv:1108.0015 [hep-ex].
[19] G.L. Fogli, E. Lisi, A. Marrone, A. Palazzo, A.M. Rotunno, Phys. Rev. D 84 (2011) 053007 arXiv:1106.6028 [hep-ph].
[20] T. Schwetz, M. Tortola, J.W.F. Valle, New J. Phys. 13 (2011) 109401 arXiv:1108.1376 [hep-ph].
[21] Y. Abe, et al. [Double Chooz Collaboration], Phys. Rev. Lett. 108 (2012) 13 arXiv:1112.6353 [hep-ex].
[22] F.P. An, et al. [Daya Bay Collaboration], Phys. Rev. Lett. 108 (2012) 171803 arXiv:1203.1669 [hep-ex].
[23] J.K. Ahn, et al. [RENO Collaboration], Phys. Rev. Lett. 108 (2012) 191802 arXiv:1204.0626 [hep-ex].
[24] D.V. Forero, M. Tortola, J.W.F. Valle, Phys. Rev. D 86 (2012) 073012 arXiv:1205.4018 [hep-ph].
[25] G.L. Fogli, E. Lisi, A. Marrone, D. Montanino, A. Palazzo, A.M. Rotunno, Phys. Rev. D 86 (2012) 013012 arXiv:1205.5254 [hep-ph].
[26] M.C. Gonzalez-Garcia, M. Maltoni, J. Salvado, T. Schwetz, J. High Energy Phys. 1212 (2012) 123 arXiv:1209.3023 [hep-ph].
[27] K. Abe, et al. [T2K Collaboration], Phys. Phys. Rev. Lett. 112 (2014) 061802 arXiv:1311.4750 [hep-ex].
[28] P. Adamson, et al. [NOvA Collaboration], Phys. Rev. Lett. 116 (15) (2016) 151806 arXiv:1601.05022 [hep-ex].
[29] K. Abe, et al. [T2K Collaboration], Phys. Rev. Lett. 118 (15) (2017) 151801 arXiv:1701.00432 [hep-ex].
[30] P. Adamson, et al. [NOvA Collaboration], Phys. Rev. Lett. 118 (23) (2017) 231801 arXiv:1703.03328 [hep-ex].
[31] I. Esteban, M.C. Gonzalez-Garcia, M. Maltoni, I. Martinez-Soler, T. Schwetz, J. High Energy Phys. 1701 (2017) 087 arXiv:1611.01514 [hep-ph].
[32] NuFIT webpage http://www.nu-fit.org (see v3.2: Three-neutrino fit based on data available in January 2018).
[33] P.F. de Salas, D.V. Forero, C.A. Ternes, M. Tortola, J.W.F. Valle, Status of neutrino oscillations 2017, arXiv:1708.01186v1 [hep-ph].
[34] F. Capozzi, E. Lisi, A. Marrone, D. Montanino, A. Palazzo, Nuclear Phys. B 908 (2016) 218 arXiv:1601.07777 [hep-ph].
[35] F. Capozzi, E. Di Valentino, E. Lisi, A. Marrone, A. Melchiorri, A. Palazzo, Phys. Rev. D 95 (9) (2017) 096014 arXiv:1703.04471 [hep-ph].
[36] G.L. Fogli, E. Lisi, Phys. Rev. D 54 (1996) 3667. hep-ph/9604415.
[37] L. Wolfenstein, Phys. Rev. D 17 (1978) 2369.
[38] S.P. Mikheev, A.Y. Smirnov, Sov. J. Nucl. Phys. 42 (1985) 913; Yad. Fiz. 42 (1985) 1441.
[39] S.P. Mikheev, A.Y. Smirnov, Nuovo Cimento C 9 (1986) 17.
[40] M. Blennow, A.Y. Smirnov, Adv. High Energy Phys. 2013 (2013) 972485 arXiv:1306.2903 [hep-ph].
[41] R.B. Patterson, Ann. Rev. Nucl. Part. Sci. 65 (2015) 177 arXiv:1506.07917 [hep-ex].
[42] E.W. Otten, C. Weinheimer, Rep. Progr. Phys. 71 (2008) 086201 arXiv:0909.2104 [hep-ex].
[43] G. Drexlin, V. Hannen, S. Mertens, C. Weinheimer, Adv. High Energy Phys. 2013 (2013) 293986 arXiv:1307.0101 [physics.ins-det].
[44] B.H.J. McKellar, Phys. Lett. B 97 (1980) 93;
F. Vissani, in: G.L. Fogli (Ed.), The Proceedings of *NOW 2000*, Europhysics Neutrino Oscillation Workshop (Conca Specchiulla, Otranto, Italy, 2000), Nuclear Phys. B (Proc. Suppl.) 100 (2001) 273;
J. Studnik, M. Zralek, Phys. Lett. B 557 (2003) 224 hep-ph/0110232. See also the discussion in Y. Farzan and A.Yu. Smirnov.
[45] A.D. Dolgov, Phys. Rep. 370 (2002) 333. hep-ph/0202122.
[46] S. Hannestad, Prog. Part. Nucl. Phys. 65 (2010) 185 arXiv:1007.0658 [hep-ph].
[47] Y.Y.Y. Wong, Ann. Rev. Nucl. Part. Sci. 61 (2011) 69 arXiv:1111.1436 [astro-ph.CO].
[48] J. Lesgourgues, S. Pastor, Adv. High Energy Phys. 2012 (2012) 608515 arXiv:1212.6154 [hep-ph].
[49] M. Lattanzi, M. Gerbino, Front. Phys. 5 (2018) 70 arXiv:1712.07109 [astro-ph.CO].
[50] E. Majorana, Nuovo Cimento 14 (1937) 171.
[51] S.T. Petcov, Adv. High Energy Phys. 2013 (2013) 852987 arXiv:1303.5819 [hep-ph].
[52] S.M. Bilenky, C. Giunti, Internat. J. Modern Phys. A 30 (2015) 1530001 arXiv:1411.4791 [hep-ph].
[53] H. Paes, W. Rodejohann, New J. Phys. 17 (11) (2015) 115010 arXiv:1507.00170 [hep-ph].
[54] S. Dell'Oro, S. Marcocci, M. Viel, F. Vissani, Adv. High Energy Phys. 2016 (2016) 2162659 arXiv:1601.07512 [hep-ph].
[55] J.D. Vergados, H. Ejiri, F. Simkovic, Internat. J. Modern Phys. E 25 (11) (2016) 1630007 arXiv:1612.02924 [hep-ph].
[56] P. Vogel, A. Piepke, Neutrinoless Double-β Decay, in [2].
[57] G. Fantini, A. Gallo Rosso, F. Vissani, V. Zema, Adv. Ser. Direct. High Energy Phys. 28 (2018) 37 arXiv:1802.05781 [hep-ph].
[58] A. Palazzo, Modern Phys. Lett. A 28 (2013) 1330004 arXiv:1302.1102 [hep-ph].
[59] S. Gariazzo, C. Giunti, M. Laveder, Y.F. Li, E.M. Zavanin, J. Phys. G 43 (2016) 033001 arXiv:1507.08204 [hep-ph].
[60] S. Gariazzo, C. Giunti, M. Laveder, Y.F. Li, J. High Energy Phys. 1706 (2017) 135 arXiv:1703.00860 [hep-ph].
[61] M. Dentler, A. Hernandez-Cabezudo, J. Kopp, P. Machado, M. Maltoni, I. Martinez-Soler, T. Schwetz, Updated global analysis of neutrino oscillations in the presence of eV-scale sterile neutrinos, arXiv:1803.10661 [hep-ph.
[62] S. Hannestad, I. Tamborra, T. Tram, J. Cosmol. Astropart. Phys. 1207 (2012) 025 arXiv:1204.5861 [astro-ph.CO].
[63] F. Forastieri, M. Lattanzi, G. Mangano, A. Mirizzi, P. Natoli, N. Saviano, J. Cosmol. Astropart. Phys. 1707 (07) (2017) 038 arXiv:1704.00626 [astro-ph.CO].
[64] M. Archidiacono, S. Gariazzo, C. Giunti, S. Hannestad, R. Hansen, M. Laveder, T. Tram, J. Cosmol. Astropart. Phys. 1608 (08) (2016) 067 arXiv:1606.07673 [astro-ph.CO].
[65] X. Chu, B. Dasgupta, J. Kopp, J. Cosmol. Astropart. Phys. 1510 (10) (2015) 011 arXiv:1505.02795 [hep-ph].
[66] Neutrino Unbound website, maintained by S. Gariazzo, C. Giunti and M. Laveder: http://nu.to.infn.it.
[67] C. Giunti, C.W. Kim, Fundamentals of Neutrino Physics and Astrophysics, Oxford U Press, Oxford, UK, 2007, p. 728.

[68] V. Barger, D. Marfatia, K.L. Whisnant, The Physics of Neutrinos, Princeton U Press, Princeton NJ, 2012, p. 224.
[69] J. Lesgourgues, G. Mangano, G. Miele, S. Pastor, Neutrino Cosmology, Cambridge U Press, Cambridge, UK, 2013, p. 392.
[70] F. Suekane, Neutrino Oscillations: A Practical Guide To Basics and Applications, in: Lecture Notes in Physics, vol. 898, Springer, Berlin and Heidelberg, Germany, 2015, p. 185.
[71] M. Spurio, Particles and Astrophysics: A Multimessenger Approach, Springer-Verlag, Berlin, Germany, 2015, p. 491.
[72] J.W.F. Valle, J. Romao, Neutrinos in High Energy and Astroparticle Physics, Wiley-VCH, Weinheim, Germany, 2015, p. 448.
[73] T. Ohlsson, (Ed.) Nuclear Phys. B 908 (2016) 466.
[74] G. Sigl, Astroparticle Physics: Theory and Phenomenology, Atlantis Press, Amsterdam, the Netherlands, 2017, p. 861.
[75] R. Aloisio, E. Coccia, F. Vissani (Eds.), Multiple Messengers and Challenges in Astroparticle Physics, Springer International Publishing, Cham, Switzerland, 2018, p. 552.
[76] A. Ereditato (Ed.), The State of the Art of Neutrino Physics: A Tutorial for Graduate Students and Young Researchers, in: Advanced Series on Directions in High Energy Physics, vol. 28, World Scientific, Singapore, 2018, p. 580.
[77] S. Bilenky, Introduction to the Physics of Massive and Mixed Neutrinos, second ed., in: Lecture Notes in Physics, vol. 947, Springer, Berlin and Heidelberg, Germany, 2018, p. 277.
[78] G.L. Fogli, E. Lisi, A. Marrone, D. Montanino, A. Palazzo, Phys. Rev. D 66 (2002) 053010. hep-ph/0206162.
[79] F. Capozzi, G.L. Fogli, E. Lisi, A. Marrone, D. Montanino, A. Palazzo, Rev. D 89 (2014) (2013) 093018 arXiv:1312.2878 [hep-ph].
[80] K. Abe, et al. [Super-Kamiokande Collaboration], Phys. Rev. D 97 (7) (2018) 072001 arXiv:1710.09126 [hep-ex].
[81] G. Bellini, et al., Phys. Rev. Lett. 107 (2011) 141302 arXiv:1104.1816 [hep-ex].
[82] G. Bellini, et al. [BOREXINO Collaboration], Nature 512 (7515) (2014) 383.
[83] M. Agostini, et al. [Borexino Collaboration], First Simultaneous Precision Spectroscopy of *pp*, ^{7}Be, and *pep* Solar Neutrinos with Borexino Phase-II, arXiv:1707.09279 [hep-ex].
[84] K. Abe, et al. [Super-Kamiokande Collaboration], Phys. Rev. D 94 (5) (2016) 052010 arXiv:1606.07538 [hep-ex].
[85] B. Aharmim, et al. [SNO Collaboration], Phys. Rev. C 88 (2013) 025501 arXiv:1109.0763 [nucl-ex].
[86] B.T. Cleveland, T. Daily, R. Davis Jr., J.R. Distel, K. Lande, C.K. Lee, P.S. Wildenhain, J. Ullman, Astrophys. J. 496 (1998) 505.
[87] J.N. Abdurashitov, et al. [SAGE Collaboration], Phys. Rev. C 80 (2009) 2002–2007 arXiv:0901.2200 [nucl-ex].
[88] F. Kaether, W. Hampel, G. Heusser, J. Kiko, T. Kirsten, Phys. Lett. B 685 (2010) 47 arXiv:1001.2731 [hep-ex].
[89] N. Vinyoles, et al., Astrophys. J. 835 (2) (2017) 202 arXiv:1611.09867 [astro-ph.SR].
[90] A. Serenelli, C. Pena-Garay, W.C. Haxton, Phys. Rev. D 87 (4) (2013) 043001 arXiv:1211.6740 [astro-ph.SR].
[91] W.T. Winter, S.J. Freedman, K.E. Rehm, J.P. Schiffer, Phys. Rev. C 73 (2006) 025503. nucl-ex/0406019.
[92] D. Frekers, et al., Phys. Rev. C 91 (2015) 034608.
[93] V. Barinov, B. Cleveland, V. Gavrin, D. Gorbunov, T. Ibragimova, Phys. Rev. D 97 (7) (2018) 073001 arXiv:1710.06326 [hep-ph].
[94] J.N. Bahcall, Neutrino Astrophysics, Cambridge U Press, Cambridge, UK, 1989, p. 592.
[95] G.L. Fogli, E. Lisi, A. Marrone, A. Palazzo, Solar neutrinos: With a tribute to John. N. Bahcall, hep-ph/0605186.
[96] A. Gando, et al. [KamLAND Collaboration], Phys. Rev. D 88 (2013) 033001 arXiv:1303.4667 [hep-ex].
[97] A. Gando, et al. [KamLAND Collaboration], Phys. Rev. D 83 (2011) 052002 arXiv:1009.4771 [hep-ex].
[98] P. Huber, Phys. Rev. C 84 (2011) 024617; Phys. Rev. C 85 (2012) 029901 (erratum). arXiv:1106.0687 [hep-ph].
[99] T.A. Mueller, et al., Phys. Rev. C 83 (2011) 054615 arXiv:1101.2663 [hep-ex].
[100] S.H. Seo [RENO Collaboration], Proceedings of Neutrino 2014, XXVI International Conference on Neutrino Physics and Astrophysics (Boston, U.S. 2014), AIP Conf. Proc. 1666 (2015) 080002 arXiv:1410.7987 [hep-ex].
[101] J.H. Choi, et al. [RENO Collaboration], Phys. Rev. Lett. 116 (21) (2016) 211801 arXiv:1511.05849 [hep-ex]
[102] Y. Abe, et al. [Double Chooz Collaboration], J. High Energy Phys. 1410 (2014) 086; J. High Energy Phys. 1502 (2015) 074 (erratum). arXiv:1406.7763 [hep-ex].
[103] F.P. An, et al. [Daya Bay Collaboration], Phys. Rev. Lett. 116 (6) (2016) 061801; Phys. Rev. Lett. 118 (9) (2017) 099902 (erratum) arXiv:1508.04233 [hep-ex]
[104] P. Novella, Adv. High Energy Phys. 2015 (2015) 364392 arXiv:1512.03366 [hep-ex].
[105] A.A. Sonzogni, T.D. Johnson, E.A. McCutchan, Phys. Rev. C 91 (1) (2015) 011301.
[106] A.C. Hayes, J.L. Friar, G.T. Garvey, D. Ibeling, G. Jungman, T. Kawano, R.W. Mills, Phys. Rev. D 92 (3) (2015) 033015 arXiv:1506.00583 [nucl-th].
[107] P. Huber, Nuclear Phys. B 908 (2016) 268 arXiv:1602.01499 [hep-ph].
[108] M. Maltoni, A.Y. Smirnov, Eur. Phys. J. A 52 (4) (2016) 87 arXiv:1507.05287 [hep-ph].
[109] M. Baak, et al. [Gfitter Group], Eur. Phys. J. C 74 (2014) 3046 arXiv:1407.3792 [hep-ph].
[110] S. Alioli, et al., Eur. Phys. J. C 77 (5) (2017) 280 arXiv:1606.02330 [hep-ph].
[111] S. Dulat, et al., Phys. Rev. D 93 (3) (2016) 033006 arXiv:1506.07443 [hep-ph].
[112] L.A. Harland-Lang, A.D. Martin, P. Motylinski, R.S. Thorne, Eur. Phys. J. C 75 (5) (2015) 204 arXiv:1412.3989 [hep-ph].
[113] R.D. Ball, et al. [NNPDF Collaboration], Eur. Phys. J. C 77 (10) (2017) 663 arXiv:1706.00428 [hep-ph].
[114] G.L. Fogli, E. Lisi, A. Palazzo, Phys. Rev. D 65 (2002) 073019. hep-ph/0105080.
[115] M.H. Ahn, et al. [K2K Collaboration], Phys. Rev. Lett. 90 (2003) 041801. hep-ex/0212007.
[116] E. Aliu, et al. [2K Collaboration], Phys. Phys. Rev. Lett. 94 (2005) 081802. hep-ex/0411038.
[117] P. Adamson, et al. [MiniBooNE and MINOS Collaborations], Phys. Rev. Lett. 102 (2009) 211801 arXiv:0809.2447 [hep-ex].
[118] P. Adamson, et al. [MINOS Collaboration], Phys. Rev. Lett. 112 (2014) 191801 arXiv:1403.0867 [hep-ex].
[119] N. Agafonova, et al. [OPERA Collaboration], Phys. Rev. Lett. 115 (12) (2015) 12 arXiv:1507.01417 [hep-ex].
[120] K. Abe, et al. [T2K Collaboration], Phys. Rev. D 96 (9) (2017) 092006 arXiv:1707.01048 [hep-ex].
[121] P. Huber, M. Lindner, W. Winter, Comput. Phys. Comm. 167 (2005) 195. hep-ph/0407333.
[122] P. Huber, J. Kopp, M. Lindner, M. Rolinec, W. Winter, Comput. Phys. Comm. 177 (2007) 432. hep-ph/0701187.
[123] M. Hartz, T2K Neutrino Oscillation Results with Data up to 2017 Summer, seminar at KEK (4 August 2017), available at https://www.t2k.org/docs/talk (talk n. 282 in the list). See also the subsequent T2K talks, up to March 2018.
[124] A. Radovic, Latest Neutrino Oscillation Results from NOvA, seminar at Fermilab (12 January 2018), available at https://www-nova.fnal.gov/NOvA_Collaboration_Information/speakers.html (first talk in the 2018 list). See also the subsequent NOvA talks, up to March 2018.
[125] G. Cowan, Statistics, in [2].
[126] Fernanda Psihas, Measurement of Long Baseline Neutrino Oscillations and Improvements from Deep Learning (Ph.D. thesis), Indiana University, U.S. Feb. 2018, available at http://nova-docdb.fnal.gov/cgi-bin/ShowDocument?docid=29108.
[127] T2K and NOvA collaborations to produce joint neutrino oscillation analysis by 2021. Full announcement (30 January 2018) available at http://t2k-experiment.org/2018/01/t2k-nova-announce/.
[128] A. Cervera, A. Donini, M.B. Gavela, J.J. Gomez Cadenas, P. Hernandez, O. Mena, S. Rigolin, Nuclear Phys. B 579 (2000) 17; Nuclear Phys. B 593 (2001) 731 (erratum) hep-ph/0002108.

[129] M. Freund, Phys. Rev. D 64 (2001) 053003. hep-ph/0103300.
[130] E.K. Akhmedov, R. Johansson, M. Lindner, T. Ohlsson, T. Schwetz, J. High Energy Phys. 0404 (2004) 078. hep-ph/0402175.
[131] A. Takamura, K. Kimura, H. Yokomakura, Phys. Lett. B 595 (2004) 414. hep-ph/0403150.
[132] H.J. He, X.J. Xu, Phys. Rev. D 95 (3) (2017) 033002 arXiv:1606.04054 [hep-ph].
[133] Y.F. Li, J. Zhang, S. Zhou, J.y. Zhu, J. High Energy Phys. 1612 (2016) 109 arXiv:1610.04133 [hep-ph].
[134] S.J. Parke, P.B. Denton, H. Minakata, Analytic Neutrino Oscillation Probabilities in Matter: Revisited, arXiv:1801.00752 [hep-ph].
[135] V. Martemyanov, L. Mikaelyan, V. Sinev, V. Kopeikin, Y. Kozlov, Phys. Atom. Nucl. 66 (2003) 1934; Yad. Fiz. 66 (2003) 1982, hep-ex/0211070.
[136] F.P. An, et al. [Daya Bay Collaboration], Phys. Rev. D 95 (7) (2017) 072006 arXiv:1610.04802 [hep-ex].
[137] H. Seo [RENO Collaboration], Proceedings of EPS-HEP 2017, European Physical Society Conference on High Energy Physics (Venice, Italy, 2017), PoS EPS-HEP 2017 (2017) 134.
[138] I. Gil Botella [Double Chooz Collaboration], Proceedings of "EPS-HEP 2017", European Physical Society Conference on High Energy Physics (Venice, Italy, 2017), PoS EPS-HEP 2017 (2017) 109.
[139] S.B. Kim, T. Lasserre, Y. Wang, Adv. High Energy Phys. (2013) 453816.
[140] P. Vogel, L. Wen, C. Zhang, Nature Commun. 6 (2015) 6935 arXiv:1503.01059 [hep-ex].
[141] X. Qian, J.C. Peng, Physics with Reactor Neutrinos, arXiv:1801.05386 [hep-ex].
[142] S.H. Seo, et al. [RENO Collaboration], Spectral Measurement of the Electron Antineutrino Oscillation Amplitude and Frequency using 500 Live Days of RENO Data, arXiv:1610.04326 [hep-ex].
[143] The First Workshop on Reactor Neutrino Experiments, (Seoul, Korea, Oct. 2016), webpage https://indico.snu.ac.kr/indico/event/4/.
[144] The "Second Reactor-θ_{13} Workshop" (APC, Paris, France, Jun. 2017), webpage https://indico.in2p3.fr/event/14578/.
[145] S.H. Seo, in: A. Marrone, A. Mirizzi, D. Montanino (Eds.), Proceedings of NOW 2016, International Neutrino Oscillation Workshop (Otranto, Italy, 2016), PoS NOW 2016 (2017) 002 arXiv:1701.06843 [hep-ex].
[146] Talk by L. Lebanowsky at NNN 2016, International Workshop on Next Generation Nucleon Decay and Neutrino Detectors (Beijing, China, Nov. 2016), available at http://nnn16.ihep.ac.cn/.
[147] Talk by Zeyuan Yu at the NuPhys 2017, International Workshop on Prospects in Neutrino Physics (London, UK, Dec. 2017), available at https://indico.ph.qmul.ac.uk/indico/event/nuphys2017.
[148] The official χ^2 map from Daya Bay [136] is available as ancillary file (DayaBay_DeltaChiSq _1230days.txt) at https://arxiv.org/abs/1610.04802.
[149] S. Parke, Phys. Rev. D 93 (5) (2016) 053008 arXiv:1601.07464 [hep-ph].
[150] F. Capozzi, E. Lisi, A. Marrone, Phys. Rev. D 89 (1) (2014) 013001 arXiv:1309.1638 [hep-ph].
[151] F. Capozzi, E. Lisi, A. Marrone, Phys. Rev. D 92 (9) (2015) 093011 arXiv:1508.01392 [hep-ph].
[152] Y. Fukuda, et al. [Super-Kamiokande Collaboration], Phys. Rev. Lett. 81 (1998) 1562. hep-ex/9807003.
[153] T. Kajita, Y. Totsuka, Rev. Modern Phys. 73 (2001) 85.
[154] S.T. Petcov, Phys. Lett. B 434 (1998) 321. hep-ph/9805262.
[155] E.K. Akhmedov, Nuclear Phys. B 538 (1999) 25. hep-ph/9805272.
[156] E.K. Akhmedov, A. Dighe, P. Lipari, A.Y. Smirnov, Nuclear Phys. B 542 (1999) 3. hep-ph/9808270.
[157] M.V. Chizhov, S.T. Petcov, Phys. Rev. D 63 (2001) 073003. hep-ph/9903424.
[158] E.K. Akhmedov, M. Maltoni, A.Y. Smirnov, J. High Energy Phys. 0705 (2007) 077. hep-ph/0612285.
[159] E.K. Akhmedov, M. Maltoni, A.Y. Smirnov, J. High Energy Phys. 0806 (2008) 072 arXiv:0804.1466 [hep-ph].
[160] S. Choubey, Nuclear Phys. B 908 (2016) 235 arXiv:1603.06841 [hep-ph].
[161] T. Kajita, E. Kearns, M. Shiozawa, the Super-Kamiokande Collaboration, Nuclear Phys. B 908 (2016) 14.
[162] G.L. Fogli, E. Lisi, D. Montanino, G. Scioscia, Phys. Rev. D 55 (1997) 4385. hep-ph/9607251.
[163] G.L. Fogli, E. Lisi, A. Marrone, G. Scioscia, Phys. Rev. D 59 (1999) 033001. hep-ph/9808205.
[164] M.C. Gonzalez-Garcia, M. Maltoni, Phys. Rep. 460 (2008) 1 arXiv:0704.1800 [hep-ph].
[165] S.F. Ge, K. Hagiwara, J. High Energy Phys. 1409 (2014) 024 arXiv:1312.0457 [hep-ph].
[166] G.L. Fogli, E. Lisi, A. Marrone, D. Montanino, Phys. Rev. D 67 (2003) 093006. hep-ph/0303064.
[167] F. Capozzi, E. Lisi, A. Marrone, Phys. Rev. D 91 (2015) 073011 arXiv:1503.01999 [hep-ph].
[168] F. Capozzi, E. Lisi, A. Marrone, J. Phys. G 45 (2) (2018) 024003 arXiv:1708.03022 [hep-ph].
[169] T.J. Irvine, Development of Neutron-Tagging Techniques and Application to Atmospheric Neutrino Oscillation Analysis in Super-Kamiokande (Ph.D. thesis), U. of Tokyo, Japan, 2014 available at http://www-sk.icrr.u-tokyo.ac.jp/sk/publications/index-e.html#doctor.
[170] M.G. Aartsen, et al. [IceCube Collaboration], Phys. Rev. D 91 (7) (2015) 072004 arXiv:1410.7227 [hep-ex].
[171] IceCube Oscillations: 3 years muon neutrino disappearance data (released 27 Jan 2015), https://icecube.wisc.edu/science/data/nu_osc.
[172] M.G. Aartsen, et al. [IceCube Collaboration], Phys. Rev. Lett. 120 (7) (2018) 071801 arXiv:1707.07081 [hep-ex].
[173] IceCube Collaboration: Measurement of atmospheric neutrino oscillations with three years of data from the full sky (χ^2 map released 13 Feb 2018), https://icecube.wisc.edu/science/data/2018nuosc.
[174] T. Schwetz, M.A. Tortola, J.W.F. Valle, New J. Phys. 10 (2008) 113011 arXiv:0808.2016 [hep-ph].
[175] R. Wendell, et al. [Super-Kamiokande Collaboration], Phys. Rev. D 81 (2010) 092004.
[176] Super-Kamiokande Collaboration: χ^2 maps derived from the oscillations analysis in [175] in the one-dominant mass-scale approximation ($\delta m^2 = 0$), http://www-sk.icrr.u-tokyo.ac.jp/sk/atmpd/sk123_subdom_data/.
[177] Super-Kamiokande Collaboration: χ^2 maps derived from the full 3ν oscillations analysis in [80] http://www-sk.icrr.u-tokyo.ac.jp/sk/publications/result-e.html.
[178] Tyce DeYoung, private communication.
[179] International Workshop on Sub-dominant oscillation effects in atmospheric neutrino experiments (Kashiwa, Japan, 2004), website http://www-rccn.icrr.u-tokyo.ac.jp/rccnws04/.
[180] Proceedings of [179], edited by T. Kajita and K. Okumura: Sub-Dominant Oscillation Effects in Atmospheric Neutrino Experiments, Frontiers Science Series vol. 45, Universal Academy Press, Tokyo, Japan, 2005.
[181] ANW'16, Atmospheric Neutrino Workshop 2016 (Garching, Germany, 2016), website https://indico.ph.tum.de/event/3533/.
[182] PANE 2018, Advanced Workshop on Physics of Atmospheric Neutrinos (Trieste, Italy, 2018), website http://indico.ictp.it/event/8312/.
[183] NEUTEL Workshop Series (since 1988) on Neutrino Telescopes in Venice. 17th edition: NEUTEL 2017 (Venice, Italy, 2017), website https://agenda.infn.it/conferenceDisplay.py?confId=11857.
[184] VLVNT Workshop Series (since 2003) on Very Large Volume Neutrino Telescopes. 8th edition: VLVNT 2018 (Dubna, Russia, 2018), website https://vlvnt2018.jinr.ru.
[185] J.P. Yanez, A. Kouchner, Adv. High Energy Phys. 2015 (2015) 271968 arXiv:1509.08404 [hep-ex].
[186] M.G. Aartsen, et al. [IceCube PINGU Collaboration], Letter of Intent: The Precision IceCube Next Generation Upgrade (PINGU), arXiv:1401.2046 [physics.ins-det].

[187] M.G. Aartsen, et al. [IceCube Collaboration], J. Phys. G 44 (5) (2017) 054006 arXiv:1607.02671 [hep-ex].
[188] S. Adrian-Martinez, et al. [KM3Net Collaboration], J. Phys. G 43 (8) (2016) 084001 arXiv:1601.07459 [astro-ph.IM].
[189] K. Abe, et al. Letter of Intent: The Hyper-Kamiokande Experiment –Detector Design and Physics Potential, arXiv:1109.3262 [hep-ex]; K. Abe, et al., Hyper-Kamiokande Design Report" arXiv:1805.04163 [physics.ins-det], See also the website http://www.hyperk.org.
[190] M.S. Athar, et al. [INO Collaboration], India-based Neutrino Observatory: Project Report, INO-2006-01. Available at http://www.ino.tifr.res.in/ino/OpenReports/report.php.
[191] S.T. Petcov, M. Piai, Phys. Lett. B 533 (2002) 94. hep-ph/0112074.
[192] F. An, et al. [JUNO Collaboration], J. Phys. G 43 (3) (2016) 030401 arXiv:1507.05613 [physics.ins-det].
[193] K. Abe, et al. [Hyper-Kamiokande Proto-Collaboration], PTEP 2015 (2015) 053C02 arXiv:1502.05199 [hep-ex].
[194] J. Strait, et al. [DUNE Collaboration], Long-Baseline Neutrino Facility (LBNF) and Deep Underground Neutrino Experiment (DUNE) : Conceptual Design Report, Volume 3: Long-Baseline Neutrino Facility for DUNE June 24, 2015, arXiv:1601.05823 [physics.ins-det].
[195] E. Wildner, et al., Adv. High Energy Phys. 2016 (2016) 8640493 arXiv:1510.00493 [physics.ins-det].
[196] M. Blennow, P. Coloma, P. Huber, T. Schwetz, J. High Energy Phys. 1403 (2014) 028 arXiv:1311.1822 [hep-ph].
[197] M.C. Gonzalez-Garcia, M. Maltoni, J. High Energy Phys. 1309 (2013) 152 arXiv:1307.3092 [hep-ph].
[198] J. Liao, D. Marfatia, K. Whisnant, Phys. Lett. B 771 (2017) 247 arXiv:1704.04711 [hep-ph].
[199] M. Ghosh, O. Yasuda, Testing NSI suggested by the solar neutrino tension in T2HKK and DUNE, arXiv:1709.08264 [hep-ph.
[200] A. Palazzo, Phys. Rev. D 83 (2011) 101701 arXiv:1101.3875 [hep-ph].
[201] A. Bolanos, O.G. Miranda, A. Palazzo, M.A. Tortola, J.W.F. Valle, Phys. Rev. D 79 (2009) 113012 arXiv:0812.4417 [hep-ph].
[202] F. Capozzi, I.M. Shoemaker, L. Vecchi, J. Cosmol. Astropart. Phys. 1707 (07) (2017) 021 arXiv:1702.08464 [hep-ph].
[203] P. Coloma, P.B. Denton, M.C. Gonzalez-Garcia, M. Maltoni, T. Schwetz, J. High Energy Phys. 1704 (2017) 116 arXiv:1701.04828 [hep-ph].
[204] P. Coloma, M.C. Gonzalez-Garcia, M. Maltoni, T. Schwetz, Phys. Rev. D 96 (11) (2017) 115007.
[205] M.M. Guzzo, A. Masiero, S.T. Petcov, Phys. Lett. B 260 (1991) 154.
[206] C. Biggio, M. Blennow, E. Fernandez-Martinez, J. High Energy Phys. 0908 (2009) 090 arXiv:0907.0097 [hep-ph].
[207] F.J. Escrihuela, O.G. Miranda, M.A. Tortola, J.W.F. Valle, Phys. Rev. D 80 (2009) 105009; Phys. Rev. D 80 (2009) 129908 (erratum). arXiv:0907.2630 [hep-ph]
[208] T. Ohlsson, Rep. Progr. Phys. 76 (2013) 044201 arXiv:1209.2710 [hep-ph].
[209] O.G. Miranda, H. Nunokawa, New J. Phys. 17 (9) (2015) 095002 arXiv:1505.06254 [hep-ph].
[210] Y. Farzan, M. Tortola, Front. Phys. 6 (2018) 10 arXiv:1710.09360 [hep-ph].
[211] M.B. Gavela, D. Hernandez, T. Ota, W. Winter, Phys. Rev. D 79 (2009) 013007 arXiv:0809.3451 [hep-ph].
[212] S. Antusch, J.P. Baumann, E. Fernandez-Martinez, Nuclear Phys. B 810 (2009) 369 arXiv:0807.1003 [hep-ph].
[213] K.S. Babu, A. Friedland, P.A.N. Machado, I. Mocioiu, J. High Energy Phys. 1712 (2017) 096 arXiv:1705.01822 [hep-ph].
[214] M. Blennow, S. Choubey, T. Ohlsson, D. Pramanik, S.K. Raut, A.combined.study.of. source, J. High Energy Phys. 1608 (2016) 090 arXiv:1606.08851 [hep-ph].
[215] K.N. Deepthi, S. Goswami, N. Nath, Phys. Rev. D 96 (7) (2017) 075023 arXiv:1612.00784 [hep-ph].
[216] S.K. Agarwalla, S.S. Chatterjee, A. Palazzo, Phys. Lett. B 762 (2016) 64 arXiv:1607.01745 [hep-ph].
[217] J. Liao, D. Marfatia, K. Whisnant, J. High Energy Phys. 1701 (2017) 071 arXiv:1612.01443 [hep-ph].
[218] S. Fukasawa, O. Yasuda, Nuclear Phys. B 914 (2017) 99 arXiv:1608.05897 [hep-ph].
[219] S.F. Ge, A.Y. Smirnov, J. High Energy Phys. 1610 (2016) 138 arXiv:1607.08513 [hep-ph].
[220] M. Masud, P. Mehta, Phys. Rev. D 94 (5) (2016) 053007 arXiv:1606.05662 [hep-ph].
[221] P. Coloma, H. Minakata, S.J. Parke, Phys. Rev. D 90 (2014) 093003 arXiv:1406.2551 [hep-ph].
[222] M. Ghosh, P. Ghoshal, S. Goswami, N. Nath, S.K. Raut, Phys. Rev. D 93 (1) (2016) 013013 arXiv:1504.06283 [hep-ph].
[223] M. Lindner, W. Rodejohann, X.J. Xu, Phys. Rev. D 97 (7) (2018) 075024 arXiv:1709.10252 [hep-ph].
[224] K.N. Abazajian, et al. Light Sterile Neutrinos: A White Paper, arXiv:1204.5379 [hep-ph].
[225] J. Spitz, Proceedings of Neutrino 2014, XXVI International Conference on Neutrino Physics and Astrophysics (Boston, U.S. 2014), AIP Conf. Proc. 1666 (2015) 180004.
[226] D. Lhuillier, Proceedings of Neutrino 2014, XXVI International Conference on Neutrino Physics and Astrophysics (Boston, U.S. 2014), AIP Conf. Proc. 1666 (2015) 180003.
[227] J. Barry, W. Rodejohann, H. Zhang, J. High Energy Phys. 1107 (2011) 091 arXiv:1105.3911 [hep-ph].
[228] S. Antusch, C. Biggio, E. Fernandez-Martinez, M.B. Gavela, J. Lopez-Pavon, J. High Energy Phys. 0610 (2006) 084. hep-ph/0607020.
[229] S. Parke, M. Ross-Lonergan, Phys. Rev. D 93 (11) (2016) 113009 arXiv:1508.05095 [hep-ph].
[230] J. Tang, Y. Zhang, Y.F. Li, Phys. Lett. B 774 (2017) 217 arXiv:1708.04909 [hep-ph].
[231] Y.F. Li, Z. z. Xing, J.y. Zhu, Indirect unitarity violation entangled with matter effects in reactor antineutrino oscillations, arXiv:1802.04964 [hep-ph].
[232] M. Blennow, P. Coloma, E. Fernandez-Martinez, J. Hernandez-Garcia, J. Lopez-Pavon, J. High Energy Phys. 1704 (153) (2017) arXiv:1609.08637 [hep-ph].
[233] C.S. Fong, H. Minakata, H. Nunokawa, Non-unitary evolution of neutrinos in matter and the leptonic unitarity test, arXiv:1712.02798 [hep-ph].
[234] Y.F. Li, S. Luo, Phys. Rev. D 93 (3) (2016) 033008 arXiv:1508.00052 [hep-ph].
[235] O.G. Miranda, M. Tortola, J.W.F. Valle, Phys. Rev. Lett. 117 (6) (2016) 061804 arXiv:1604.05690 [hep-ph].
[236] N. Klop, A. Palazzo, Phys. Rev. D 91 (7) (2015) 073017 arXiv:1412.7524 [hep-ph].
[237] A. Palazzo, Phys. Lett. B 757 (2016) 142 arXiv:1509.03148 [hep-ph].
[238] F. Capozzi, C. Giunti, M. Laveder, A. Palazzo, Phys. Rev. D 95 (3) (2017) 033006 arXiv:1612.07764 [hep-ph].
[239] S.K. Agarwalla, S.S. Chatterjee, A. Palazzo, Phys. Rev. Lett. 118 (3) (2017) 031804 arXiv:1605.04299 [hep-ph].
[240] S.K. Agarwalla, S.S. Chatterjee, A. Dasgupta, A. Palazzo, J. High Energy Phys. 1602 (2016) 111 arXiv:1601.05995 [hep-ph].
[241] D. Dutta, P. Ghoshal, S.K. Sehrawat, Phys. Rev. D 95 (9) (2017) 095007 arXiv:1610.07203 [hep-ph].
[242] G.L. Fogli, E. Lisi, A. Marrone, A. Melchiorri, A. Palazzo, P. Serra, J. Silk, Phys. Rev. D 70 (2004) 113003. hep-ph/0408045.
[243] G.L. Fogli, E. Lisi, A. Marrone, A. Melchiorri, A. Palazzo, P. Serra, J. Silk, A. Slosar, Phys. Rev. D 75 (2007) 053001. hep-ph/0608060.
[244] K.A. Olive, Sum of neutrino masses, in [2].
[245] J. Lesgourgues, L. Verde, Neutrinos in Cosmology, in [2].
[246] M. Gerbino, M. Lattanzi, O. Mena, K. Freese, Phys. Lett. B 775 (2017) 239 arXiv:1611.07847 [astro-ph.CO].
[247] S. Gariazzo, M. Archidiacono, P.F. de Salas, O. Mena, C.A. Ternes, M. Tortola, J. Cosmol. Astropart. Phys. 1803 (03) (2018) 011 arXiv:1801.04946 [hep-ph].
[248] A. Caldwell, A. Merle, O. Schulz, M. Totzauer, Phys. Rev. D 96 (7) (2017) 073001 arXiv:1705.01945 [hep-ph].
[249] M. Agostini, G. Benato, J. Detwiler, Phys. Rev. D 96 (5) (2017) 053001 arXiv:1705.02996 [hep-ex].
[250] R.N. Mohapatra, et al., Rep. Progr. Phys. 70 (2007) 1757. hep-ph/0510213.

[251] A. Gando, et al. [KamLAND-Zen Collaboration], Phys. Rev. Lett. 117 (8) (2016) 082503; Phys. Rev. Lett. 117 (10) (2016) 109903 (addendum). arXiv:1605.02889 [hep-ex].
[252] J.B. Albert, et al. [EXO Collaboration], Phys. Rev. Lett. 120 (7) (2018) 072701 arXiv:1707.08707 [hep-ex].
[253] C. Alduino, et al. [CUORE Collaboration], Phys. Rev. Lett. 120 (13) (2018) 132501 arXiv:1710.07988 [nucl-ex].
[254] C.E. Aalseth, et al. [Majorana Collaboration], Phys. Rev. Lett. 120 (13) (2018) 132502 arXiv:1710.11608 [nucl-ex].
[255] M. Agostini, et al. [GERDA Collaboration], Phys. Rev. Lett. 120 (2018) 132503 arXiv:1803.11100 [nucl-ex].
[256] J. Engel, J. Menendez, Rep. Progr. Phys. 80 (4) (2017) 046301 arXiv:1610.06548 [nucl-th].
[257] F. Iachello, J. Kotila, J. Barea, Proceedings of Neutel 2015, XVI International Workshop on Neutrino Telescopes (Venice, Italy, 2015), PoS NEUTEL 2015 (2015) 047.
[258] J.T. Suhonen, Front. Phys. 5 (2017) 55 arXiv:1712.01565 [nucl-th].
[259] E. Lisi, A. Rotunno, F. Simkovic, Phys. Rev. D 92 (9) (2015) 093004 arXiv:1506.04058 [hep-ph].
[260] N. Aghanim, et al. [Planck Collaboration], Astron. Astrophys. 594 (2016) A11 arXiv:1507.02704 [astro-ph.CO].
[261] N. Aghanim, et al. [Planck Collaboration], Astron. Astrophys. 596 (2016) A107 arXiv:1605.02985 [astro-ph.CO].
[262] F. Beutler, et al., Mon. Not. R. Astron. Soc. 416 (2011) 3017 arXiv:1106.3366 [astro-ph.CO].
[263] A.J. Ross, L. Samushia, C. Howlett, W.J. Percival, A. Burden, M. Manera, Mon. Not. R. Astron. Soc. 449 (1) (2015) 835 arXiv:1409.3242 [astro-ph.CO].
[264] L. Anderson, et al. [BOSS Collaboration], Mon. Not. R. Astron. Soc. 441 (1) (2014) 24 arXiv:1312.4877 [astro-ph.CO].
[265] P.A.R. Ade, et al. [Planck Collaboration], Astron. Astrophys. 594 (2016) A15 arXiv:1502.01591 [astro-ph.CO].
[266] J. Angrik, et al. [KATRIN Collaboration], KATRIN Design Report 2004 (245 pages), Report FZKA-7090, NPI ASCR Rez EXP-01/2005, MS-KP-0501. Available at the website: www.katrin.kit.edu.
[267] R.G.H. Robertson, in: P. Bernardini, G.L. Fogli, E. Lisi (Eds.), Proceedings of now 2014, International Neutrino Oscillation Workshop (Otranto, Italy, 2014), Nucl. Part. Phys. Proc. 265–266 (2015) 7 arXiv:1502.00144 [nucl-ex].
[268] S. Mertens, Proceedings of NuPhys 2015, International Workshop on Prospects in Neutrino Physics (London, UK, 2015), J. Phys. Conf. Ser. 718 (2) (2016) 022013 arXiv:1605.01579 [nucl-ex].
[269] L. Gastaldo, in: A. Marrone, A. Mirizzi, D. Montanino (Eds.), Proceedings of now 2016, International Neutrino Oscillation Workshop (Otranto, Italy, 2016), PoS now 2016 (2017) 060.